

September 8, 2014

A supersimple analysis of $e^-e^+ \rightarrow ZH$ at high energy.

G.J. Gounaris^a and F.M. Renard^b

^aDepartment of Theoretical Physics, Aristotle University of Thessaloniki,
Gr-54124, Thessaloniki, Greece.

^bLaboratoire Univers et Particules de Montpellier, UMR 5299
Université Montpellier II, Place Eugène Bataillon CC072
F-34095 Montpellier Cedex 5.

Abstract

We study the process $e^-e^+ \rightarrow ZH$ where H represents the standard model (SM) Higgs particle H_{SM} , or the MSSM ones h^0 and H^0 . In each case, we compute the one-loop effects and establish very simple expressions, called supersimple (sim), for the helicity conserving (dominant) and the helicity violating (suppressed) amplitudes. Such expressions, are then used to construct various cross sections and asymmetries, involving polarized or unpolarized beams and Z-polarization measurements. We examine the adequacy of such expressions to distinguish SM or MSSM effects, from other types of BSM (beyond the standard model) contributions.

PACS numbers: 12.15.-y, 12.60.-i, 13.66.Fg

1 Introduction

Our basic motivation for this study is that after the Higgs boson [1] discovery [2], precise analyses of Higgs properties are necessary in order to confirm its origin and nature; SM, SUSY, other extensions, compositeness, ... etc. Such searches will be done in several places and with various processes [3], in particular at the future ILC [4].

Our aim here is to look for simple tests, using experimental measurements at high energies, which could immediately distinguish SM or MSSM (minimal supersymmetric standard model) contributions, from possible additional (small) anomalous BSM effects.

For various processes observable at LHC or ILC, we have already shown that one loop effects can be described, at sufficiently high energies, by simple expressions which reflect in a clear way the nature of the underlying dynamics. We have called these expressions "supersimple" (sim) and we have already derived them for $e^-e^+ \rightarrow t\bar{t}$, $e^-e^+ \rightarrow W^-W^+$ and other processes [5, 6, 7, 8, 9]. In all cases, these simple expressions can help distinguishing SM or MSSM, from other BSM (beyond the standard model) dynamics.

In this paper we concentrate on $e^-e^+ \rightarrow ZH$. This process has been considered as the most important one for studying the Higgs boson at e^-e^+ colliders [10]. As we point out below, there are several points that may be added to the previous analyses of this process, even in the SM case [10].

In the next sections we examine the contents of the Born and one loop amplitudes for this process. At the Born level, we verify that the helicity conserving (HC) amplitudes (those involving longitudinal Z -states) are the dominant ones at high energies, behaving like constants; while the helicity violating (HV) amplitudes (those involving transverse Z -states) are high-energy-suppressed, but only like m_Z/\sqrt{s} . This is in agreement with the asymptotic helicity conservation rule, which claims (to all orders), that the HC amplitudes are the only ones that may be asymptotically non-vanishing [5, 6].

At the one loop level, the aforementioned high energy behaviour of the various amplitudes, is only modified by \ln - and \ln^2 -terms accompanied by constant terms. The coefficients of these terms possibly involve ratios of Mandelstam variables. This way, we establish the aforementioned "sim" expressions. Such expressions clearly emphasize the dynamics behind the high energy values of the various helicity amplitudes.

We first work in the SM case. Particularly for the HC amplitudes, it is instructive to see how the sim expressions are realized through cancelations among various contributions, and how its various terms combine to produce the Sudakov forms expected by the general rules [11]. For achieving this, it is advantageous to use the equivalence theorem relating the longitudinal Z amplitudes to the Goldstone $e^+e^- \rightarrow G^0H$ ones, not only at tree-level [12], but also to all orders in SM or MSSM [13].

For the HV $e^+e^- \rightarrow ZH$ amplitudes, the rather weak m_Z/\sqrt{s} Born suppression, is considerably modified by \ln and \ln^2 one-loop corrections. Therefore, at intermediately high energies, we cannot completely neglect the one-loop corrections for them, as we have done for $e^-e^+ \rightarrow t\bar{t}$, W^-W^+ [8, 9]. Therefore, sim expressions for them are also needed. It turns out that these one-loop corrections are more complicated than those for the HC

ones, reflecting the fact that there is no Sudakov rule for the HV amplitudes [11].

In a second step we consider the MSSM cases $e^-e^+ \rightarrow Zh^0$ and $e^-e^+ \rightarrow ZH^0$. Apart from a simple mixing factor for the Higgs coupling (which strongly suppresses the H^0 amplitudes) the corresponding Born terms are similar to those of the SM case. At one loop level though, there are specific supersymmetric contributions, involving sfermions, inos and additional Higgses. We establish the corresponding MSSM sim expressions for the HC and HV amplitudes and we compare them with those of the SM case.

Finally, as the HV amplitudes always give only small contributions to the various observables, it is sufficient to use simple fits for them, which we present in subsection B.1

In a final step we compare the SM and MSSM effects, based on either the exact one-loop or sim expressions for the various amplitudes. In addition the SM effects are compared to those of a tree-level BSM contribution created by some anomalous HZZ and $HZ\gamma$ couplings [14].

To this aim, we study whether the sim expressions may be sufficient for a good description of various $e^-e^+ \rightarrow ZH$ observables, in either SM or MSSM. As such, we consider cross sections involving unpolarized e^\mp -beams, as well as forward-backward and polarization asymmetries constructed by using polarized e^- -beams and/or measuring the final Z -polarization. It turns out that some of these observables may be useful, not only for distinguishing SM from a BSM model like the one mentioned above, but they may also be sensitive to SM - MSSM differences.

The contents of the paper is the following. In Sect.2 we give the expressions for the Born helicity amplitudes for H_{SM}, h^0, H^0 production. In Sect.3 we present the one-loop effects in the on-shell renormalization scheme. Their sim expressions are introduced in Sect.4 for all HC and HV amplitudes, while the complete results are given in Appendices A and B. In Sect.5 we give an example of an effective BSM contribution created by some anomalous couplings of the Standard Model Higgs particle. The possibility of a complete amplitude analysis using various unpolarized and polarized observables is described in Sect.6; while the corresponding numerical analysis, including illustrations, is given in Sect.7. Sect.8 contains the conclusions on the possibility of discriminating SM or MSSM from some types of BSM corrections. The accuracy of the sim expressions in SM and MSSM is also discussed.

2 Kinematics, Born helicity amplitudes

We consider the process

$$e^-_{\lambda}(l) e^+_{\lambda'}(l') \rightarrow Z_{\tau}(p) H(p') \quad , \quad (1)$$

where (λ, λ') denote the helicities of the incoming (e^-, e^+) states, and τ the helicity of the outgoing Z with its polarization vector being ϵ . H represents either H_{SM}, h^0 or H^0 . As shown in (1), (l, l', p, p') are the various particle momenta satisfying $l + l' = p + p'$. We

also use

$$s = (l + l')^2, \quad t = (l - p)^2, \quad u = (l - p')^2, \quad p_Z = \beta_Z \frac{s}{2}, \quad (2)$$

where $p_Z = \sqrt{E_Z^2 - m_Z^2}$ denotes the Z -three-momentum in the ZH -rest frame. Finally, the angle between the incoming e^- momentum l and the outgoing Z momentum p , in the center of mass frame, is denoted as θ .

In the standard model (SM) and its minimal supersymmetric extension MSSM, the Born amplitude

$$A^{\text{Born}} = - \frac{e^2 f_{ZZH}}{(s - m_Z^2)} I_1 [g_{eL}^Z P_L + g_{eR}^Z P_R], \quad (3)$$

is only due to s-channel Z exchange. Since the electron mass is neglected, the only possible invariant form it can contain is

$$I_1 = \bar{v}(e_{\lambda'}^+) \not{\epsilon} u(e_{\lambda}^-). \quad (4)$$

The relevant couplings in (3) are

$$g_{eL}^Z = \frac{-1 + 2s_W^2}{2s_W c_W}, \quad g_{eR}^Z = \frac{s_W}{c_W}, \quad (5)$$

$$f_{ZZH_{SM}} = \frac{m_Z}{s_W c_W}, \quad f_{ZZh^0} = \frac{m_Z}{s_W c_W} \sin(\beta - \alpha), \quad f_{ZZH^0} = \frac{m_Z}{s_W c_W} \cos(\beta - \alpha), \quad (6)$$

where the first term in (6) applies to SM, while the rest to MSSM.

Since, the neglect of the electron mass implies

$$\lambda = -\lambda' = \mp \frac{1}{2}, \quad (7)$$

and $(\tau = \pm 1, 0)$, there exist six independent helicity amplitudes, denoted as $F_{\lambda\tau}(\theta)$, in the usual Jacob-Wick convention [15]. In case CP is conserved though, the exact relation

$$F_{\lambda,\tau}(\theta) = F_{\lambda,-\tau}(\pi - \theta), \quad (8)$$

reduces them to only four independent ones.

At the Born level, these are the transverse- Z amplitudes ($\lambda = \pm 1/2, \tau = \pm 1$)

$$F_{\lambda,\tau}^{\text{Born}}(\theta) = - \frac{e^2 f_{ZZH} \sqrt{s}}{\sqrt{2}(s - m_Z^2)} \left[g_{eL}^Z (\tau \cos \theta - 1) \delta_{\lambda,-} - g_{eR}^Z (\tau \cos \theta + 1) \delta_{\lambda,+} \right], \quad (9)$$

and the longitudinal- Z amplitudes ($\lambda = \pm 1/2, \tau = 0$)

$$F_{\lambda,0}^{\text{Born}}(\theta) = \frac{e^2 f_{ZZH} E_Z \sqrt{s} \sin \theta}{m_Z (s - m_Z^2)} \left[g_{eL}^Z \delta_{\lambda,-} - g_{eR}^Z \delta_{\lambda,+} \right]. \quad (10)$$

Note that the high energy Helicity Conservation (HCns) rule [5, 6] requires

$$\lambda + \lambda' = \tau \quad , \quad (11)$$

which, combined with (7), implies that the transverse amplitudes in (9) violate HCns, and are indeed suppressed like m_Z/\sqrt{s} , according to (9). We call them HV (helicity violating) amplitudes.

Contrary to this, the longitudinal- Z amplitudes in (10), which satisfy (11) and are called HC (helicity conserving), tend to constants at high energies, given by

$$F_{\lambda,0}^{\text{Born}} \rightarrow \frac{e^2 f_{ZZH} \sin \theta}{2m_Z} \left[g_{eL}^Z \delta_{\lambda,-} - g_{eR}^Z \delta_{\lambda,+} \right] \quad . \quad (12)$$

We have checked that this result agrees with the direct computation of the Goldstone process $e^- e^+ \rightarrow G^0 H$, and the asymptotic relation $F^{\text{Born}}(Z_{\text{long}} H) = i F^{\text{Born}}(G^0 H)$ implied by the equivalence theorem in [12, 13].

3 Electroweak corrections at one loop

In all explicit amplitude expressions presented in Sect.3,4, we assume for simplicity that CP symmetry is respected in¹ SM and MSSM, implying according to (8), four independent helicity amplitudes, two HC amplitudes and two HV ones.

The corresponding one-loop amplitudes arise from ZZ and γZ self-energies and counter terms generating renormalized initial and final vertices, triangles (initial and final in s -channel, and up and down in t and u channels), direct, crossed and twisted boxes and specific diagrams involving 4-leg bosonic couplings, see [10]. In the MSSM case additional diagrams exist involving supersymmetric partners like sleptons, squarks, charginos, neutralinos and additional Higgses. We have recomputed all these contributions in terms of Passarino-Veltman (PV) functions [16], which are then expanded, as explained in the next section, in order to obtain simple high energy expressions.

All one loop contributions appear in 4 invariant forms: the I_1 -form, already appearing at Born level and given in (4), and the 4 new ones

$$\begin{aligned} I_2 &= \bar{v}(e_{\lambda'}^+) \epsilon \cdot p' \not{p} u(e_{\lambda}^-) \quad , \quad I_3 = \bar{v}(e_{\lambda'}^+) \epsilon \cdot l' \not{p} u(e_{\lambda}^-) \quad , \\ I_4 &= \bar{v}(e_{\lambda'}^+) \epsilon \cdot l \not{p} u(e_{\lambda}^-) \quad , \quad J_1 = -i \bar{v}(e_{\lambda'}^+) \epsilon^{\mu\nu\rho\sigma} \gamma_{\mu} \epsilon_{\nu} p'_{\rho} p_{\sigma} u(e_{\lambda}^-) \quad , \end{aligned} \quad (13)$$

the last of which J_1 would only appear in the case of CP-violating couplings; see Sect.5.

Concerning the counter terms, we note that they are calculated in the so-called on-shell scheme [17], leading to the usual forms for the renormalized initial Zee - and the final ZZH -vertices. We assume that the mass of the final Higgs bosons are well determined,

¹The possibility of CP violating effects are only considered with respect of a BSM model in Sect.5.

such that one can apply the corresponding residue and demixing constraints leading to a contribution $\delta Z_H/2$ factorizing the Born term. In the SM case, we thus get

$$\delta Z_{H_{SM}} = -\Sigma'_H(M_{H_{SM}}^2) \quad . \quad (14)$$

Correspondingly in MSSM, where $(H_1 = h^0, H_2 = H^0)$, we have

$$\frac{1}{2}\delta Z_{H_i} = -\frac{1}{2} \left[\Sigma'_{H_i H_i}(M_{H_i}^2) + \sum_j \frac{f_{ZZH_j}}{f_{ZZH_i}} \frac{[\Sigma_{H_j H_i}^*(M_{H_i}^2) - \Sigma_{H_i H_j}(M_{H_j}^2)]}{(M_{H_j}^2 - M_{H_i}^2)} \right] + \delta c_{H_i} \quad , \quad (15)$$

where

$$\delta c_{H_1} = \frac{\delta \sin(\beta - \alpha)}{\sin(\beta - \alpha)} \quad , \quad \delta c_{H_2} = \frac{\delta \cos(\beta - \alpha)}{\sin(\beta - \alpha)} \quad , \quad (16)$$

with α being the usual neutral Higgs mixing angle. Using the purely divergent β renormalization, the quantities in (16) may be calculated using [18]

$$\frac{\delta \tan \beta}{\tan \beta} = \frac{\alpha \Delta}{16\pi s_W^2 m_W^2} \Sigma_f N_f \left(\frac{m_f^2}{\cos^2 \beta} \delta_{f,\text{up}} - \frac{m_f^2}{\sin^2 \beta} \delta_{f,\text{down}} \right) \quad , \quad (17)$$

while α is kept fixed at the value given by the benchmark choice. We have checked the cancellation of the divergences in such a scheme. The counter terms in (14-17) are expressed in terms of the un-renormalized self-energies $\Sigma_{H_i H_j}$, Σ_{ZZ} , $\Sigma_{\gamma Z}$ that can be found in [8, 9, 19].

4 Supersimple (sim) expressions

For deriving these simple expressions one starts from the exact one-loop results in terms of Passarino-Veltman (PV) functions, and then uses their high energy expansions given in [20]. The sim-results thus obtained for the HC amplitudes are given in Appendix A, while the corresponding ones for the HV amplitudes appear in Appendix B.

Before discussing these results, we first note that the infrared divergencies are regularized by introducing a photon mass m_γ . As usual, these divergencies are canceled by adding to $d\sigma(e^-e^+ \rightarrow ZH)/d\cos\theta$, the cross section for bremsstrahlung of an unobservable soft photon contribution given by [10]

$$\frac{d\sigma_{\text{brems}}}{d\cos\theta} = \frac{d\sigma^{\text{Born}}}{d\cos\theta} \delta_{\text{brems}}(m_\gamma, \Delta E) \quad , \quad (18)$$

with

$$\delta_{\text{brems}}(m_\gamma, \Delta E) = -\frac{\alpha}{\pi} \left\{ 2 \left(1 - \ln \frac{s}{m_e^2} \right) \ln \left(\frac{2\Delta E}{m_\gamma} \right) + \frac{1}{2} \ln^2 \frac{m_e^2}{s} + \ln \frac{m_e^2}{s} + \frac{\pi^2}{3} \right\} \quad , \quad (19)$$

where ΔE describes the highest energy of the emitted unobservable soft photon satisfying

$$m_\gamma \leq \Delta E \ll \sqrt{s} \quad . \quad (20)$$

When (18) is added to $d\sigma(e^-e^+ \rightarrow ZH)/d\cos\theta$ (for the same polarizations of the initial e^\mp -beams or the final Z boson), it completely cancels the infrared-photon part, irrespective of the actual value of m_γ , provided that it can be treated as infinitesimal. As in [9, 7, 8], we always chose $m_\gamma = m_Z$, which satisfies (20) at the high energies we are interested in, and considerably simplifies the results in Appendices A and B.

This way, the infrared divergencies may be handled, not only in the differential cross sections, but also in the various asymmetries defined in Sect.6.

We next turn to the HC and HV amplitudes:

(a) The HC amplitudes:

For the HC amplitudes, which are the leading ones at high energy, we follow the procedure used in [7, 8, 9]. In the process $e^-e^+ \rightarrow ZH$, these HC amplitudes are the 2 longitudinal Z amplitudes whose Born expressions are given in (10). At the one-loop level though, the direct derivation of the high energy expressions is very delicate, because of huge gauge cancelations among individual terms growing like \sqrt{s}/m_Z . But the derivation is facilitated by working with the amplitudes of the Goldstone process $e^-e^+ \rightarrow G^0H$, which are equivalent up to m^2/s corrections [13].

This way, one obtains the sim expressions in Appendix A. Explicitly, for the SM case, these are given by the results (A.5, A.6). Correspondingly, for the MSSM cases of $H = h^0$ and $H = H^0$, the results are given in (A.8, A.9). These expressions clearly indicate the important dynamical contents.

As in [7, 8, 9], these high energy expression consist of combinations of the two augmented Sudakov terms exemplified in (A.1, A.2), and the two energy and mass independent forms (A.4, A.3). Such expressions provide precise high energy predictions, where only quantities vanishing like powers of energy are neglected.

(b) The HV amplitudes

The HV amplitudes involve transverse-Z states, which at Born level are given by (9). Assuming for simplicity CP invariance for the SM or MSSM contributions, then the constraint (B.1) implies the existence of only two independent amplitudes. As such we take F_{--} , F_{+-} given in (B.2, B.3) at the one-loop order. Since these amplitudes are only suppressed like m/\sqrt{s} at high energy, they are not negligible at intermediate energies, in both SM and MSSM. To obtain satisfactory expressions for them at intermediate energies, we start from the direct one loop expressions in terms of the PV functions, which we subsequently expanded. The resulting expressions are less compact than those in the HC cases, because of more involved mass dependent terms. The reason for this is due to the non-existence of any Sudakov rule for such mass-suppressed amplitudes [11]. This way we obtain the expressions (B.5-B.10) in SM, and (B.13-B.16) in MSSM, which must be used in conjunction with (B.2, B.3) mentioned above.

These expressions are quite complicated. Nevertheless, since the HV amplitudes are much less important than the HC ones, it is possible to obtain sufficiently accurate fits for them by neglecting mass differences in the various loop contributions (most importantly

the logarithms) and only consider a common mass scale for them. Such fits are given in (B.19) and Table B.2, expressed in terms of squared log, linear log and constant contributions.

5 Other BSM effects

BSM effects like anomalous Higgs couplings to vector bosons may be described by effective operators, like e.g. in [14]. Here we just want to see how one can differentiate such effects from the one loop SM contributions, and whether the accuracy of the sim expressions are adequate for that purpose.

For a simple illustration we take the 2 CP-conserving operators O_{UB} , O_{UW} , and the 2 CP-violating ones \bar{O}_{UB} , \bar{O}_{UW} of [14] with couplings d_{UB} , d_{UW} , \bar{d}_{UB} , \bar{d}_{UW} , inducing the anomalous $\gamma Z H_{SM}$ - and $ZZ H_{SM}$ -couplings

$$\begin{aligned} d_{\gamma Z} &= s_W c_W (d_{UB} - d_{UW}) \quad , \quad d_{ZZ} = d_{UB} c_W^2 + d_{UW} s_B^2 \quad , \\ \bar{d}_{\gamma Z} &= s_W c_W (\bar{d}_{UB} - \bar{d}_{UW}) \quad , \quad \bar{d}_{ZZ} = \bar{d}_{UB} c_W^2 + \bar{d}_{UW} s_B^2 \quad . \end{aligned} \quad (21)$$

Combining them with the SM Zee couplings given in (5) and the γee couplings $g_{eL}^\gamma = g_{eR}^\gamma = q_e = -1$, we obtain the tree level BSM contributions to the invariant amplitudes

$$A(e^- e^+ \rightarrow Z H_{SM}) = - \sum_{V=Z,\gamma} \frac{e^2}{(s - m_V^2)} [g_1^V I_1 + g_2^V I_2 + g_3^V J_1] [g_{eL}^V P_L + g_{eR}^V P_R] \quad , \quad (22)$$

where the I_1 , I_2 , J_1 forms are defined in (4, 13), while the corresponding effective couplings are

$$\begin{aligned} g_1^\gamma &= - \frac{2E_Z \sqrt{s}}{m_Z s_W c_W} d_{\gamma Z} \quad , \quad g_1^Z = \frac{2E_Z \sqrt{s}}{m_Z s_W c_W} d_{ZZ} \quad , \\ g_2^\gamma &= - \frac{2}{m_Z s_W c_W} d_{\gamma Z} \quad , \quad g_2^Z = \frac{2}{m_Z s_W c_W} d_{ZZ} \quad , \\ g_3^\gamma &= - \frac{2}{m_Z s_W c_W} \bar{d}_{\gamma Z} \quad , \quad g_3^Z = \frac{2}{m_Z s_W c_W} \bar{d}_{ZZ} \quad . \end{aligned} \quad (23)$$

The last line in (23) indicates that the presence of CP-violating BSM physics would induce a J_1 contribution coming from a Z or photon exchange.

For illustrating BSM contributions somehow comparable to the SM ones at energies below 5 TeV, we use values of the effective couplings in (23), of the order of 0.0005. Such BSM corrections, denoted as "eff", appear in several figures below.

6 Observables and amplitude analysis

In the case that no CP-conservation constraint is available, there exist six independent $e^- e^+ \rightarrow ZH$ helicity amplitudes, which means that at least six independent observables

are needed. If CP conservation holds, this number reduces to four.

Such observables may be defined by using the two different initial e^\pm polarizations and the three possible final Z polarizations. In constructing them, we first note the differential unpolarized cross section

$$\frac{d\sigma}{d\cos\theta} = \frac{\beta_Z}{128\pi s} \sum_{\lambda\tau} |F_{\lambda\tau}(\theta)|^2 \quad , \quad (24)$$

and its integrated over all angles cross section

$$\sigma = \int_{-1}^1 d\cos\theta \frac{d\sigma}{d\cos\theta} \quad , \quad (25)$$

where β_Z is defined in (2), and one sums over $\lambda = \pm\frac{1}{2}$ and $\tau = \pm 1, 0$. Cross sections could also be integrated over the forward (with respect to the e^- -beam) or the backward region, leading to σ_F and σ_B respectively.

Another possibility of unpolarized beam cross sections, is when the helicity of the final Z is also observed. The integrated cross section in this case are denoted as $\sigma^{Z\tau}$ with $(\tau = -1, 0, +1)$. Similarly $\sigma_F^{Z\tau}$ and $\sigma_B^{Z\tau}$ may also be considered.

Finally, the integrated cross section for initially polarized e^- beams, in the case the Z -helicity is not observed, is denoted as $\sigma_{L,R}$ for the cases $\lambda = -\frac{1}{2}$ and $\lambda = +\frac{1}{2}$ respectively.

In principle we can also consider more detail measurements where polarized e^- -beams are used and the Z helicity is simultaneously measured. The integrated cross section may then be denoted as $\sigma(\lambda, \tau)$ and related useful definitions are

$$\begin{aligned} \sigma(\lambda, \tau) &\Rightarrow \sigma\left(-\frac{1}{2}, \tau\right) \equiv \sigma_L(\tau) \quad , \quad \sigma\left(\frac{1}{2}, \tau\right) \equiv \sigma_R(\tau) \quad , \\ \sigma(\lambda, \tau = -1) &\equiv \sigma^{Z-}(\lambda) \quad , \quad \sigma(\lambda, \tau = 1) \equiv \sigma^{Z+}(\lambda) \quad , \\ \sigma(\lambda, \tau = 0) &\equiv \sigma^{Z0}(\lambda) \quad . \end{aligned} \quad (26)$$

Apart from the unpolarized differential cross section in (24) and the angularly integrated ones, we next enumerate some in principle observable asymmetries, for unpolarized or polarized beams. These are:

- Initial e^- -left-right polarization asymmetries, for the case that the Z polarization is not looked at

$$A_{LR} = \frac{\sigma_L - \sigma_R}{\sigma_L + \sigma_R} \quad , \quad (27)$$

or separately for the three cases where the Z helicity is also measured

$$A_{LR}(\tau) = \frac{\sigma_L(\tau) - \sigma_R(\tau)}{\sigma_L(\tau) + \sigma_R(\tau)} \equiv \frac{\sigma_L^{Z\tau} - \sigma_R^{Z\tau}}{\sigma_L^{Z\tau} + \sigma_R^{Z\tau}} \quad , \quad (28)$$

where $\tau = \pm 1, 0$.

- Left-Right asymmetries obtained by restricting angular integrations in the forward direction,

$$A_{LR}^F(\tau) = \frac{\sigma_{LF}(\tau) - \sigma_{RF}(\tau)}{\sigma_{LF}(\tau) + \sigma_{RF}(\tau)} \equiv \frac{[\sigma_L^{Z\tau} - \sigma_R^{Z\tau}]_F}{[\sigma_L^{Z\tau} + \sigma_R^{Z\tau}]_F} , \quad (29)$$

and correspondingly in the backward direction.

- Final Z transverse polarization asymmetry for unpolarized e^\mp beams

$$A^{\text{pol } Z} = \frac{\sigma^{Z-} - \sigma^{Z+}}{\sigma^{Z-} + \sigma^{Z+}} , \quad (30)$$

and for a definite e^- -helicity λ

$$A^{\text{pol } Z}(\lambda) = \frac{\sigma^{Z-}(\lambda) - \sigma^{Z+}(\lambda)}{\sigma^{Z-}(\lambda) + \sigma^{Z+}(\lambda)} \equiv \frac{\sigma(\lambda, \tau = -1) - \sigma(\lambda, \tau = +1)}{\sigma(\lambda, \tau = -1) + \sigma(\lambda, \tau = +1)} . \quad (31)$$

- Forward-backward asymmetries, in the unpolarized beam case

$$A_{FB} = \frac{\sigma_F - \sigma_B}{\sigma} , \quad (32)$$

or

$$A_{FB}(\lambda, \tau) = \frac{\sigma_F(\lambda, \tau) - \sigma_B(\lambda, \tau)}{\sigma(\lambda, \tau)} , \quad (33)$$

for any definite e^- and Z polarizations.

- Combining (30-33), one also obtains a peculiar forward-backward asymmetry of the above Z transverse polarization asymmetry,

$$A_{FB}^{\text{pol } Z} = \frac{(\sigma^{Z-} - \sigma^{Z+})_F - (\sigma^{Z-} - \sigma^{Z+})_B}{\sigma^{Z-} + \sigma^{Z+}} , \quad (34)$$

for unpolarized e^\pm beams, and

$$A_{FB}^{\text{pol } Z}(\lambda) = \frac{[\sigma^{Z-}(\lambda) - \sigma^{Z+}(\lambda)]_F - [\sigma^{Z-}(\lambda) - \sigma^{Z+}(\lambda)]_B}{\sigma^{Z-}(\lambda) + \sigma^{Z+}(\lambda)} , \quad (35)$$

for any definite electron helicity $\lambda = L, R$. It turns out that the asymmetries in (34, 35) are very useful for disentangling SM, MSSM and BSM corrections.

In case CP is conserved, then (8) would relate the forward and backward cross sections by

$$\sigma_F(\lambda, \tau) = \sigma_B(\lambda, -\tau) , \quad (36)$$

implying through (33) the following conditions:

•

$$A_{FB}(\lambda, -\tau) = -A_{FB}(\lambda, \tau) \quad , \quad (37)$$

which remains true also for unpolarized e^\mp -beams, where one sums over $\lambda = \mp 1/2$, obtaining

$$A_{FB}(-\tau) = -A_{FB}(\tau) \Rightarrow A_{FB}(Z_+) = -A_{FB}(Z_-) \quad , \quad A_{FB}(Z_0) = 0 \quad . \quad (38)$$

If the Z polarization is not measured, then (38) leads to $A_{FB} = 0$.

•

$$A_{LR}^F(\tau) = A_{LR}^B(-\tau) \quad , \quad (39)$$

induced by the Left-Right asymmetries in the forward and backward directions and the definition (29). This means

$$A_{LR}^F(Z_-) = A_{LR}^B(Z_+) \quad , \quad A_{LR}^F(Z_0) = A_{LR}^B(Z_0) \quad . \quad (40)$$

• And the condition

$$A_F^{\text{pol } Z}(\lambda) = -A_B^{\text{pol } Z}(\lambda) \quad , \quad (41)$$

arising from (31, 36), for any $\lambda = L, R$. Note that the totally integrated asymmetry $A^{\text{pol } Z}(\lambda)$ vanishes.

In the next section we illustrate the above properties for CP conserving one loop corrections to SM or MSSM models; as well for effective, possibly CP violating anomalous couplings of the SM Higgs particle. It turns out that some of the above asymmetries are particularly sensitive to the dynamical details, and may be very useful for disentangling SM, BSM and MSSM.

7 Numerical analysis

For the MSSM illustrations , we use benchmarks S1 and S2 of [21]. In both of them, the EW scale values of all squark masses are at the 2 TeV level, $A_t = A_b = 2.3$ TeV and

$$\mu = 0.4 \quad , \quad M_1 = 0.25 \quad , \quad M_2 = 0.5 \quad , \quad M_3 = 2 \quad , \quad (42)$$

where all masses are in TeV. These two benchmarks differ only in the leptonic and Higgs-sector EW scale parameters given by

$$\begin{aligned} \text{S1} &\Rightarrow m_{\tilde{l}} = A_\tau = 0.5 \quad , \quad m_{A^0} = 0.5 \quad , \quad \tan \beta = 20 \quad , \\ \text{S2} &\Rightarrow m_{\tilde{l}} = A_\tau = 0.75 \quad , \quad m_{A^0} = 1. \quad , \quad \tan \beta = 30 \quad . \end{aligned} \quad (43)$$

Such benchmarks are consistent with present LHC constraints [21].

The computations and various comparisons have been made for both benchmarks S1 and S2. The resulting amplitudes are very similar, the differences being at the order of 0.5%. So we only present illustrations for the the S1 case.

7.1 Comparison of basic amplitudes

We first look at the 6 Born helicity amplitudes versus energy, at angle 60° . Fig.1 shows these Born amplitudes for $e^-e^+ \rightarrow HZ$ in SM, and for $e^-e^+ \rightarrow h^0Z$ and $e^-e^+ \rightarrow H^0Z$ in the MSSM benchmark S1 mentioned above [21]. As seen there, the HV amplitudes are suppressed compared to the HC ones at high energies (above 1 TeV), but they become comparable to them shortly below 1TeV.

Note that the H^0 SUSY amplitudes are very small for the S1 benchmark, due to the coupling factor $\cos(\beta - \alpha) \simeq 0$ in [21]. This process will probably be unobservable (cross sections will be about 10^{-5} times smaller than for h^0), and it will not be useful to consider the one loop corrections. Only strong anomalous couplings could lead to observable effects, in such a case.

We then present the one loop results for the six amplitudes in $e^-e^+ \rightarrow ZH$ (Fig.2) for SM, and $e^-e^+ \rightarrow Zh^0$ (Fig.3) for MSSM. In both cases, the results are plotted versus energy at an angle 60° , and compared to their sim and Born approximations. In the SM case (Fig.2), we also show how the various amplitudes would look like in the case that an additional effective anomalous coupling of 0.0005, as described in Sect.5, also exists.

Comparing the upper rows of Figs.2, 3, with the middle and lowest ones, one recognizes the large logarithmic (Sudakov) one-loop corrections to the Born amplitudes in the HC cases; for the HV amplitudes, these corrections are relatively smaller. In the SM case (Fig.2), the sim accuracy is quite good, already at around 1 TeV. In the h^0 case (Fig.3) though, the accuracy is only at the few percent level at 1 TeV, but it improves quickly as the various supersymmetric thresholds are overpassed and the energy approaches 5 TeV.

As seen in Fig.2, such a sim accuracy may be sufficient for discriminating the SM contributions to both the the HC and HV amplitudes, from a BSM contribution, like the one described by the anomalous couplings in Sect.5. For achieving this, it assumed of course that an amplitude analysis of the experimental data, like the one sketched Sect.6, is successfully performed. In our illustrations we use constant effective couplings, leading to BSM contributions strongly growing with the energy. Obviously such contributions could be tempered above some given basic scale, by form factors.

We now turn to the various observable introduced in Sect. 6 and study their effects in SM, BSM and MSSM.

7.2 Unpolarized differential cross sections

Fig.4 shows the unpolarized differential cross section for $e^-e^+ \rightarrow ZH$ in SM (left panels) and for $e^-e^+ \rightarrow Zh^0$ in MSSM (right panels), first versus the energy at 60° (upper panels), and then versus $\cos \theta$ at 1 TeV (middle) and at 5 TeV (lowest) panels. The various panels intend to compare the Born, exact one loop and the sim approximation. In the left panels the possible effect of an additional effective anomalous interaction is also shown.

Note that cross sections become largest at angles around 90° , due to the $\sin \theta$ dependence of the leading Born HC amplitudes in (10). The 1 loop contribution is of the order

of 20% at 1 TeV, and increasing with the energy. The sim approximation is already good at 1 TeV and becomes better at higher energies.

7.3 Differential Asymmetries

Fig.5 shows A_{LR} , defined in (27) using polarized e^\mp beams, for $e^-e^+ \rightarrow ZH$ in SM (left panels) and $e^-e^+ \rightarrow Zh^0$ in MSSM (right panels), for the cases that the Z polarization is not looked at. Upper panels describe the energy dependence at 60° , while the middle and lower panels show the angular distributions at 1 and 5 TeV respectively.

At the Born level, $A_{LR}^{\text{Born}} \simeq 0.14$, with the actual constant value determined by the factor $[(g_{eL}^Z)^2 - (g_{eR}^Z)^2]/[(g_{eL}^Z)^2 + (g_{eR}^Z)^2]$. In all cases, the one loop contribution is quite large, as compared to Born one, for all energies and angles. The sim approximation is good at high energy, but becomes worse as the energy decreases.

We next turn to A_{LR} defined in (28), where, in addition to using polarized e^\mp -beams, the Z helicity is also measured. Figs.6,7,8 describe $e^-e^+ \rightarrow ZH$ in SM (left panels) and $e^-e^+ \rightarrow Zh^0$ in MSSM (right panels), for Z -helicities $\tau = 0, -1, +1$ respectively. The upper panels give the energy dependencies at 60° , while the middle and lower panels give the angular dependencies at 1 and 5 TeV respectively. Comparing the complete one-loop results with the Born contributions, we realize that the one-loop corrections are important.

In the $\tau = 0$ case shown in Fig.6, the Born value of A_{LR} is again $\simeq 0.14$, and strongly affected by one loop corrections. In agreement with the CP rule (39), the angular dependence is forward-backward symmetric.

In the $\tau = \mp 1$ cases shown in Figs.7 and 8, the Born contributions appear almost forward-backward antisymmetric; see middle and lower panels. This is due to the terms $(1 \pm \cos \theta)$ in (9) and to their coefficients g_{eL}^Z and g_{eR}^Z being almost opposite. We also note that for CP invariant interactions $A_{LR}(Z^+)$ and $A_{LR}(Z^-)$ are Forward-Backward symmetric to each other, see (39).

When the Z -polarization is not looked at, all these $\tau = 0$ and $\tau = \mp 1$ effects of course disappear, and the global A_{LR} appears forward-backward symmetric; see Fig.5.

These implications of the different A_{LR} measurements would produce interesting tests of the nature of the various contributions. The accuracy of sim is again good for high energies above 1 TeV.

7.4 $A^{\text{pol } Z}$ and $A^{\text{pol } Z}(\lambda)$ asymmetries.

Fig.9 shows $A^{\text{pol } Z}$ defined in (30) for unpolarized e^\mp -beams, while Fig.10 shows $A^{\text{pol } Z}(\lambda)$ defined in (31) for polarized e^\mp -beams with electron helicity $\lambda = L, R$. Left panels correspond to the SM prediction for $e^-e^+ \rightarrow ZH$, and right panels to the MSSM result for $e^-e^+ \rightarrow Zh^0$. Upper panels give the energy dependence at 60° , while middle and lower panels present the angular distributions at 1 and 5 TeV respectively.

It may be interesting to note that at Born level one has

$$A^{\text{pol } Z \text{ Born}}(\lambda) = -A^{\text{pol } Z \text{ Born}}(-\lambda) \quad , \quad (44)$$

because of the simple Z exchange with a \not{e} coupling. At one loop level though, this is no more the case, because of various diagrams differing for e_L^- and for e_R^- . If CP is conserved, as is the case for SM and the S1 benchmark [21], $A^{\text{pol } Z}(L)$ and $A^{\text{pol } Z}(R)$ are both forward-backward antisymmetric; see (41). But as their Born parts are opposite and cancel each-other, $A^{\text{pol } Z}$ is finally smaller than $A^{\text{pol } Z}(R)$ or $A^{\text{pol } Z}(L)$ separately. Consequently $A^{\text{pol } Z}$ it is very sensitive to one loop contributions, as shown in Fig.9. For these reasons, the sim accuracy, although already good at 1 TeV for $A^{\text{pol } Z}(L, R)$, needs higher energies for $A^{\text{pol } Z}$; compare Fig.10 with Fig.9.

So finally the comparison of the various polarized asymmetries in the spirit of the relations written in Sect.6 should produce fruitful tests of the natures of the corrections to the Born terms and in particular of their CP conservation property.

7.5 Integrated Asymmetries

The above illustrations show the angular dependencies at given energy. In order to accumulate more statistics we can make angular integrations, over all forward or backward angles, or only appropriate domain of angles.

As a non trivial example we give in Table 1 the asymmetries $A_{FB}^{\text{pol } Z}(L)$, $A_{FB}^{\text{pol } Z}(R)$ and $A_{FB}^{\text{pol } Z}$, in SM and S1 [21], integrated in the forward region at 5 TeV; compare (34, 35). As seen there, the individual L, R contributions are similar but of opposite sign. When

Table 1: The asymmetries $A_{FB}^{\text{pol } Z}(L)$, $A_{FB}^{\text{pol } Z}(R)$ and $A_{FB}^{\text{pol } Z}$, in SM and S1 [21], integrated in the forward region at 5 TeV.

	SM: H			MSSM S1: h^0		
	Born	one loop	sim	Born	one loop	sim
$A_{FB}^{\text{pol } Z}(L)$	0.74	0.72	0.73	0.74	0.71	0.72
$A_{FB}^{\text{pol } Z}(R)$	-0.74	-0.73	-0.73	-0.74	-0.73	-0.73
$A_{FB}^{\text{pol } Z}$	0.11	-0.22	-0.21	0.11	-0.20	-0.21

they are combined though, in the unpolarized e^\mp -beam case, a larger sensitivity to the one loop corrections appears. Table 1 confirms what has been seen at angular level in Figs.9,10. Note that the supersimple expressions reproduce correctly the exact one loop contributions.

Turning to CP conservation tests, one may also experimentally check the relations for $A_{FB}(\lambda, \tau)$, $A_{LR}^F(\tau)$ and $A^{\text{pol } Z}(\lambda)$, written respectively in (37, 40, 41). In particular the vanishing of A_{FB} when the e^\mp -beams are not polarized and the Z polarization is not measured, and the vanishing of $A^{\text{pol } Z}(\lambda)$ when integrated over all angles, are rather striking.

Summarizing, we have shown in this Section 7, that the polarized asymmetries are very powerful for identifying small corrections to Born contributions, both in SM and in MSSM cases. In addition the comparison of these various asymmetries in the spirit of the relations written in Sect.6, should produce fruitful tests of CP conservation for these corrections.

8 Conclusions and possible developments

We have analyzed in detail the Born and one loop corrections to the amplitudes for the process $e^-e^+ \rightarrow ZH$ in SM and $e^-e^+ \rightarrow Zh^0$ in MSSM, at high energies. We have separately discussed the behavior of the helicity conserving and of the helicity violating amplitudes, and we have shown that they can be reasonably approximated by simple expressions, called supersimple (sim), both in SM and in MSSM cases.

In the case of the HC amplitudes, the simplicity arises from gauge cancelations of contributions coming from various diagrams, and in addition, for MSSM, from typical cancelations between standard and partner contributions, as we have already observed in previous "supersimplicity" studies [7, 8, 9]. The sim expressions thus obtained, allow to immediately see the dynamical contents and to make a quick estimate of the size of the amplitudes. We have illustrated how much and in which high energy domain these expressions are useful.

While doing this study we have noticed several interesting properties of the process $e^-e^+ \rightarrow ZH$, for $H = H_{SM}, h^0, H^0$, and we have emphasized the importance of doing a complete amplitude analysis. It can be obtained by using the various observables i.e. the cross section measurements for different e^\pm and Z polarizations. We have illustrated the large sensitivity of the asymmetries A_{LR} , $A^{\text{pol } Z}$, $A_{FB}^{\text{pol } Z}$ to the one loop contributions. These asymmetries should allow to singularize and identify the nature (SM or MSSM or other BSM) of the corrections to Born predictions.

This work should be useful to the working groups on the various projects of high energy e^-e^+ colliders, for studying the identification of the nature of the Higgs boson and of its interactions.

Appendix A: The one-loop sim expressions for the HC amplitudes in SM and MSSM

As has been observed in [7, 9], there exist only four different forms that appear in the sim expressions. These are the two augmented Sudakov forms²

$$\overline{\ln s_{ij}(a)} \equiv \ln \frac{-s - i\epsilon}{m_i m_j} + b_0^{ij}(m_a^2) - 2 \quad (\text{A.1})$$

$$\overline{\ln^2 s_{Via}} \equiv \ln^2 \frac{-s - i\epsilon}{m_V^2} + 4L_{aVi} \quad , \quad (\text{A.2})$$

where explicit expressions for $b_0^{ij}(m_a^2)$ and L_{aVi} are given in e.g. Eqs.(A.6, A.5) of [9]. In them, quantity a describes an on-shell particle, (i, j) denote internal exchanges, and V an internal Vector (gauge) exchange; the existence of non-vanishing tree-order vertices for aij and aVi is assumed.

The other two forms entering the sim expressions, involve ratios of the Mandelstam-variables s, t, u . Denoting any of them by x, y , these ratios are given by

$$r_{xy} \equiv \frac{-x - i\epsilon}{-y - i\epsilon} \quad , \quad (\text{A.3})$$

and the two relevant forms by

$$\overline{\ln^2 r_{xy}} = \ln^2 r_{xy} + \pi^2 \quad , \quad \ln r_{xy} \quad . \quad (\text{A.4})$$

Using the definitions introduced in Sect.2, the complete sim expressions, to the one-loop order, for the various HC amplitudes in SM are

$$\begin{aligned} F_{-0} = & F_{-0}^{\text{Born}} \left\{ 1 + \frac{\alpha}{4\pi} \left\{ \frac{1}{4s_W^2 c_W^2} \left[-\overline{\ln^2 s_{Zee}} + 3\overline{\ln s_{Ze}(e)} - 1 \right] \right. \right. \\ & + \frac{1}{2s_W^2 (2s_W^2 - 1)} \left[-\overline{\ln^2 s_{W\nu e}} + 3\overline{\ln s_{W\nu}(e)} - 1 \right] \\ & - \frac{c_W^2}{s_W^2 (2s_W^2 - 1)} \left[\overline{\ln s_{W\nu}(e)} + 1 + 4\overline{\ln s_{WW}(Z)} \right] \\ & - \frac{c_W^2}{2s_W^2 (2s_W^2 - 1)} \left[\frac{1}{2} \overline{\ln^2 s_{WZH}} + \overline{\ln s_{WW}(H)} + \overline{\ln s_{WW}(Z)} \right] \\ & - 3 \left[\frac{m_t^2 \ln s_{tt}(Z)}{2s_W^2 m_W^2} + \frac{m_b^2 \ln s_{bb}(Z)}{2s_W^2 m_W^2} \right] \\ & \left. + \frac{1}{2s_W^2 (2s_W^2 - 1)} \left[-\overline{\ln^2 s_{WZH}} + 2\overline{\ln s_{WW}(H_{SM})} + 2\overline{\ln s_{WW}(Z)} \right] \right\} \end{aligned}$$

² The augmented Sudakov definitions used in this paper are more precise than those used in our previous work, but fully consistent with them.

$$\begin{aligned}
& + \frac{1}{4s_W^2 c_W^2} \left[- \overline{\ln^2 s_{ZWH}} + \overline{2\ln s_{ZZ}(H)} + \overline{2\ln s_{HZ}(Z)} \right] \\
& + \frac{c_W^2}{8s_W^2(2s_W^2 - 1)} \left[\overline{2\ln^2 s_{WZH}} + \overline{8\ln^2 t_{WZH}} + \overline{8\ln^2 u_{WZH}} - \overline{2\ln t_{WW}(H)} \right. \\
& - \overline{2\ln u_{WW}(H)} - \overline{2\ln t_{WW}(Z)} - \overline{2\ln u_{WW}(Z)} \\
& - \frac{4(u-t)}{u} \overline{\ln^2 r_{ts}} - \frac{4(t-u)}{t} \overline{\ln^2 r_{us}} + \overline{4\ln r_{ts}} + \overline{4\ln r_{us}} \left. \right] \Big\} \\
& + \frac{2s_W c_W}{(2s_W^2 - 1)} \frac{\hat{\Sigma}_{\gamma Z}(s)}{s} - \frac{\hat{\Sigma}_{ZZ}(s)}{s} + C_P \Big\} , \tag{A.5}
\end{aligned}$$

$$\begin{aligned}
F_{+0} = & F_{+0}^{\text{Born}} \left\{ 1 + \frac{\alpha}{4\pi} \left\{ \frac{1}{c_W^2} \left[- \overline{\ln^2 s_{Zee}} + \overline{3\ln s_{Ze}(e)} - 1 \right] \right. \right. \\
& + \frac{1}{2s_W^2} \left[- \overline{\ln^2 s_{WZH}} + \overline{2\ln s_{WW}(H)} + \overline{2\ln s_{WW}(Z)} \right] \\
& + \frac{1}{4s_W^2 c_W^2} \left[- \overline{\ln^2 s_{ZWH}} + \overline{2\ln s_{ZZ}(H)} + \overline{2\ln s_{HSMZ}(Z)} \right] \\
& \left. \left. - 3 \left[\frac{m_t^2 \overline{\ln s_{tt}(Z)}}{2s_W^2 m_W^2} + \frac{m_b^2 \overline{\ln s_{bb}(Z)}}{2s_W^2 m_W^2} \right] \right\} + \frac{c_W}{s_W} \frac{\hat{\Sigma}_{\gamma Z}(s)}{s} - \frac{\hat{\Sigma}_{ZZ}(s)}{s} \right\} . \tag{A.6}
\end{aligned}$$

where $\hat{\Sigma}$ denotes renormalized self-energies³, and C_P is the "pinch term" [22]

$$C_P = \frac{\alpha}{\pi} \frac{c_W^2}{s_W^2(2s_W^2 - 1)} \overline{\ln s_{WW}(Z)} . \tag{A.7}$$

The corresponding complete sim expressions for the MSSM HC amplitudes with $H = h^0, H^0$ are

$$\begin{aligned}
F_{-0} = & F_{-0}^{\text{Born}} \left\{ 1 + \frac{\alpha}{4\pi} \left\{ \frac{1}{4s_W^2 c_W^2} \left[- \overline{\ln^2 s_{Zee}} + \overline{3\ln s_{Ze}(e)} - 1 \right] \right. \right. \\
& + \frac{1}{2s_W^2(2s_W^2 - 1)} \left[- \overline{\ln^2 s_{W\nu e}} + \overline{3\ln s_{W\nu}(e)} - \sum_i |Z_{1i}^+|^2 \overline{\ln s_{\chi_i \tilde{\nu}_{eL}}(e)} \right] \\
& - \frac{c_W^2}{s_W^2(2s_W^2 - 1)} \left[\overline{\ln s_{W\nu}(e)} + \overline{4\ln s_{WW}(Z)} - \sum_i |Z_{1i}^+|^2 \overline{\ln s_{\chi_i \tilde{\nu}_{eL}}(e)} \right] \\
& - \sum_i \frac{|Z_{1i}^N s_W + Z_{2i}^N c_W|^2}{4s_W^2 c_W^2} \left[\overline{\ln s_{\chi_i \tilde{e}_L}(e)} - 1 \right] \\
& \left. \left. - \frac{c_W^2}{4s_W^2(2s_W^2 - 1)} \left[\overline{\ln^2 s_{WZH}} + \overline{2\ln s_{WW}(H)} + \overline{2\ln s_{WW}(Z)} \right] \right\} \right\} .
\end{aligned}$$

³See e.g. [8, 9]

$$\begin{aligned}
& + \frac{1}{2s_W^2(2s_W^2 - 1)} \left[-\overline{\ln^2 s_{WZH}} + 2\overline{\ln s_{WW}(H)} + 2\overline{\ln s_{WW}(Z)} \right] \\
& - 3 \left[\frac{m_t^2 \overline{\ln s_{tt}(Z)}}{2s_W^2 m_W^2} \left(h^0 \rightarrow \frac{\cos \alpha}{\sin \beta \sin(\beta - \alpha)}, H^0 \rightarrow \frac{\sin \alpha}{\sin \beta \cos(\beta - \alpha)} \right) \right. \\
& + \frac{m_b^2 \overline{\ln s_{bb}(Z)}}{2s_W^2 m_W^2} \left(h^0 \rightarrow -\frac{\sin \alpha}{\cos \beta \sin(\beta - \alpha)}, H^0 \rightarrow \frac{\cos \alpha}{\cos \beta \cos(\beta - \alpha)} \right) \Big] \\
& + \frac{1}{s_W^2} \sum_{ijk} X_{ijk}(H) \overline{\ln s_{jk}(Z)} \left(h^0 \rightarrow \frac{1}{\sin(\beta - \alpha)}, H^0 \rightarrow \frac{1}{\cos(\beta - \alpha)} \right) \\
& + \frac{1}{2s_W^2 c_W^2} \sum_{ijk} X_{ijk}^0(H) \overline{\ln s_{jk}(Z)} \left(h^0 \rightarrow \frac{1}{\sin(\beta - \alpha)}, H^0 \rightarrow \frac{1}{\cos(\beta - \alpha)} \right) \\
& + \frac{c_W^2}{8s_W^2(2s_W^2 - 1)} \left[\overline{\ln^2 s_{WZH}} + 8\overline{\ln^2 t_{WZH}} - 2\overline{\ln t_{WW}(H)} - 2\overline{\ln t_{WW}(Z)} \right. \\
& + \overline{\ln^2 s_{WZH}} + 8\overline{\ln^2 u_{WZH}} - 2\overline{\ln u_{WW}(H)} - 2\overline{\ln u_{WW}(Z)} \\
& - \frac{4(u-t)}{u} \overline{\ln^2 r_{ts}} - \frac{4(t-u)}{t} \overline{\ln^2 r_{us}} + 4\overline{\ln r_{ts}} + 4\overline{\ln r_{us}} \Big] \\
& + \frac{c_W^2}{2s_W^2(2s_W^2 - 1)} \left[\frac{s}{2u} \overline{\ln^2 r_{ts}} + \frac{s}{2t} \overline{\ln^2 r_{us}} \right] \left(h^0 \rightarrow \frac{-\cos \beta \sin \alpha}{\sin(\beta - \alpha)}, H^0 \rightarrow \frac{\cos \beta \cos \alpha}{\cos(\beta - \alpha)} \right) \\
& - \frac{(2s_W^2 - 1)}{4s_W^2 c_W^2} \left[\frac{s}{2u} \overline{\ln^2 r_{ts}} + \frac{s}{2t} \overline{\ln^2 r_{us}} \right] \left(h^0 \rightarrow \frac{\sin(\beta + \alpha)}{\sin(\beta - \alpha)}, H^0 \rightarrow \frac{-\cos(\beta + \alpha)}{\cos(\beta - \alpha)} \right) \\
& + \frac{1}{4s_W^2 c_W^2} AZ(H) \Big\} + \frac{2s_W c_W}{(2s_W^2 - 1)} \frac{\hat{\Sigma}_{\gamma Z}(s)}{s} - \frac{\hat{\Sigma}_{ZZ}(s)}{s} + C_P \Big\} , \tag{A.8}
\end{aligned}$$

$$\begin{aligned}
F_{+0} &= F_{+0}^{\text{Born}} \left\{ 1 + \frac{\alpha}{4\pi} \left\{ \frac{1}{c_W^2} \left[-\overline{\ln^2 s_{Zee}} + 3\overline{\ln s_{Ze}(e)} - 1 \right] \right. \right. \\
& + \frac{1}{2s_W^2} \left[-\overline{\ln^2 s_{WZH}} + 2\overline{\ln s_{WW}(H)} + 2\overline{\ln s_{WW}(Z)} \right] \\
& - \sum_i \frac{|Z_{1i}^N|^2}{c_W^2} \left[\overline{\ln s_{\chi_i \bar{e}_R}(e)} - 1 \right] + \frac{1}{4s_W^2 c_W^2} AZ(H) \\
& - 3 \left[\frac{m_t^2 \overline{\ln s_{tt}(Z)}}{2s_W^2 m_W^2} \left(h^0 \rightarrow \frac{\cos \alpha}{\sin \beta \sin(\beta - \alpha)}, H^0 \rightarrow \frac{\sin \alpha}{\sin \beta \cos(\beta - \alpha)} \right) \right. \\
& + \frac{m_b^2 \overline{\ln s_{bb}(Z)}}{2s_W^2 m_W^2} \left(h^0 \rightarrow -\frac{\sin \alpha}{\cos \beta \sin(\beta - \alpha)}, H^0 \rightarrow \frac{\cos \alpha}{\cos \beta \cos(\beta - \alpha)} \right) \Big] \\
& + \frac{1}{s_W^2} \sum_{ijk} X_{ijk}(H) \overline{\ln s_{jk}(Z)} \left(h^0 \rightarrow \frac{1}{\sin(\beta - \alpha)}, H^0 \rightarrow \frac{1}{\cos(\beta - \alpha)} \right) \\
& + \frac{1}{2s_W^2 c_W^2} \sum_{ijk} X_{ijk}^0(H) \overline{\ln s_{jk}(Z)} \left(h^0 \rightarrow \frac{1}{\sin(\beta - \alpha)}, H^0 \rightarrow \frac{1}{\cos(\beta - \alpha)} \right) \Big\}
\end{aligned}$$

$$\begin{aligned}
& -\frac{1}{2c_W^2} \left[\frac{s}{2u} \overline{\ln^2 r_{ts}} + \frac{s}{2t} \overline{\ln^2 r_{us}} \right] \left(h^0 \rightarrow \frac{-\sin(\beta + \alpha)}{\sin(\beta - \alpha)}, \frac{H^0 \rightarrow \cos(\beta + \alpha)}{\cos(\beta - \alpha)} \right) \Big\} \\
& + \frac{c_W}{s_W} \frac{\hat{\Sigma}_{\gamma Z}(s)}{s} - \frac{\hat{\Sigma}_{ZZ}(s)}{s} \Big\} , \tag{A.9}
\end{aligned}$$

where the renormalized gauge self energies $\hat{\Sigma}$ and the pinch term (A.7) have been used. The exact expressions for $AZ(H)$ for $H = h^0, H^0$ used in (A.8,A.9) are

$$\begin{aligned}
AZ(h^0) &= \sin^2(\beta - \alpha) A_{h^0 h^0} + \cos^2(\beta - \alpha) A_{H^0 h^0} \\
&\quad + \cos^2(\beta - \alpha) (A_{Ah^0 h^0} - A_{AH^0 h^0}) \\
AZ(H^0) &= \sin^2(\beta - \alpha) A_{h^0 H^0} + \cos^2(\beta - \alpha) A_{H^0 H^0} \\
&\quad + \sin^2(\beta - \alpha) (A_{AH^0 H^0} - A_{Ah^0 H^0}) , \tag{A.10}
\end{aligned}$$

with

$$\begin{aligned}
A_{h^0 h^0} &= -\overline{\ln^2 s_{Zh^0 h^0}} + \overline{2\ln s_{ZZ}(h^0)} + \overline{2\ln s_{Zh^0}(Z)} , \\
A_{H^0 h^0} &= -\overline{\ln^2 s_{ZH^0 h^0}} + \overline{2\ln s_{ZZ}(h^0)} + \overline{2\ln s_{ZH^0}(Z)} , \\
A_{Ah^0 h^0} &= -\overline{\ln^2 s_{ZAh^0}} + \overline{2\ln s_{AZ}(h^0)} + \overline{2\ln s_{Zh^0}(Z)} , \\
A_{Ah^0 H^0} &= -\overline{\ln^2 s_{ZAH^0}} + \overline{2\ln s_{AZ}(h^0)} + \overline{2\ln s_{ZH^0}(Z)} , \\
A_{h^0 H^0} &= -\overline{\ln^2 s_{Zh^0 H^0}} + \overline{2\ln s_{ZZ}(H^0)} + \overline{2\ln s_{Zh^0}(Z)} , \\
A_{H^0 H^0} &= -\overline{\ln^2 s_{ZH^0 H^0}} + \overline{2\ln s_{ZZ}(H^0)} + \overline{2\ln s_{ZH^0}(Z)} , \\
A_{Ah^0 H^0} &= -\overline{\ln^2 s_{ZAh^0}} + \overline{2\ln s_{AZ}(H^0)} + \overline{2\ln s_{Zh^0}(Z)} , \\
A_{AH^0 H^0} &= -\overline{\ln^2 s_{ZAH^0}} + \overline{2\ln s_{AZ}(H^0)} + \overline{2\ln s_{ZH^0}(Z)} . \tag{A.11}
\end{aligned}$$

When the mass differences among (h^0, H^0, A^0, Z) , which determine the scales of the various augmented Sudakov terms in (A.10, A.11), are neglected we obtain

$$AZ(h^0) \simeq AZ(H^0) \simeq -\overline{\ln^2 s} + 4\overline{\ln s} . \tag{A.12}$$

with a common mass scale M .

Similarly, the $X_{ijk}^0(H), X_{ijk}(H)$ expressions in (A.8,A.9) are given by the following equations, where the last lines give the approximate results in case the (h^0, H^0, A^0, Z) -mass differences are negligible:

$$\begin{aligned}
X_{ijk}^0(h^0) &= -\frac{1}{2} \left[(Z_{4i}^{N*} Z_{4k}^N - Z_{3i}^{N*} Z_{3k}^N) \left\{ \left[(-\cos \beta Z_{3k}^{N*} - \sin \beta Z_{4k}^{N*}) (Z_{1j}^{N*} s_W - Z_{2j}^{N*} c_W) \right. \right. \right. \\
&\quad \left. \left. + (j \rightarrow k) \right] (-\sin \alpha Z_{3i}^N - \cos \alpha Z_{4i}^N) (Z_{1j}^N s_W - Z_{2j}^N c_W) + (i \rightarrow j) \right\} \\
&\quad \left. - (Z_{3i}^N Z_{3k}^{N*} - Z_{4i}^N Z_{4k}^{N*}) \left\{ \left[(-\cos \beta Z_{3j}^N - \sin \beta Z_{4j}^N) (Z_{1k}^N s_W - Z_{2k}^N c_W) \right. \right. \right.
\end{aligned}$$

$$\begin{aligned}
& + (j \rightarrow k) \Big] (-\sin \alpha Z_{3j}^{N*} - \cos \alpha Z_{4j}^{N*})(Z_{1i}^{N*} s_W - Z_{2i}^{N*} c_W) + (i \rightarrow j) \Big\} \Big] \\
& \simeq -\sin(\beta - \alpha) \quad , \tag{A.13}
\end{aligned}$$

$$\begin{aligned}
X_{ijk}^0(H^0) &= -\frac{1}{2} \Big[(Z_{4i}^{N*} Z_{4k}^N - Z_{3i}^{N*} Z_{3k}^N) \Big\{ \Big[(-\cos \beta Z_{3k}^{N*} - \sin \beta Z_{4k}^{N*})(Z_{1j}^{N*} s_W - Z_{2j}^{N*} c_W) \\
& + (j \rightarrow k) \Big] (\cos \alpha Z_{3i}^N - \sin \alpha Z_{4i}^N)(Z_{1j}^N s_W - Z_{2j}^N c_W) + (i \rightarrow j) \Big\} \\
& - (Z_{3i}^N Z_{3k}^{N*} - Z_{4i}^N Z_{4k}^{N*}) \Big\{ \Big[(-\cos \beta Z_{3j}^N - \sin \beta Z_{4j}^N)(Z_{1k}^N s_W - Z_{2k}^N c_W) \\
& + (j \rightarrow k) \Big] (\cos \alpha Z_{3j}^{N*} - \sin \alpha Z_{4j}^{N*})(Z_{1i}^{N*} s_W - Z_{2i}^{N*} c_W) + (i \rightarrow j) \Big\} \Big] \\
& \simeq -\cos(\beta - \alpha) \quad , \tag{A.14}
\end{aligned}$$

$$\begin{aligned}
X_{ijk}(h^0) &= [Z_{1i}^- Z_{1k}^{-*} + \delta_{ik}(c_W^2 - s_W^2)](\cos \beta Z_{2k}^- Z_{1j}^+ - \sin \beta Z_{1k}^- Z_{2j}^+)(-\sin \alpha Z_{2i}^{-*} Z_{1j}^{+*} \\
& + \cos \alpha Z_{1i}^{-*} Z_{2j}^{+*}) - [Z_{1i}^{+*} Z_{1k}^+ + \delta_{ik}(c_W^2 - s_W^2)](\cos \beta Z_{2j}^{-*} Z_{1k}^{+*} \\
& - \sin \beta Z_{1j}^{-*} Z_{2k}^{+*})(-\sin \alpha Z_{2j}^- Z_{1i}^+ + \cos \alpha Z_{1j}^- Z_{2i}^+) \\
& \simeq -\sin(\beta - \alpha) \quad , \tag{A.15}
\end{aligned}$$

$$\begin{aligned}
X_{ijk}(H^0) &= [Z_{1i}^- Z_{1k}^{-*} + \delta_{ik}(c_W^2 - s_W^2)](\cos \beta Z_{2k}^- Z_{1j}^+ - \sin \beta Z_{1k}^- Z_{2j}^+)(\cos \alpha Z_{2i}^{-*} Z_{1j}^{+*} \\
& + \sin \alpha Z_{1i}^{-*} Z_{2j}^{+*}) - [Z_{1i}^{+*} Z_{1k}^+ + \delta_{ik}(c_W^2 - s_W^2)](\cos \beta Z_{2j}^{-*} Z_{1k}^{+*} \\
& - \sin \beta Z_{1j}^{-*} Z_{2k}^{+*})(\cos \alpha Z_{2j}^- Z_{1i}^+ + \sin \alpha Z_{1j}^- Z_{2i}^+) \\
& \simeq -\cos(\beta - \alpha) \quad . \tag{A.16}
\end{aligned}$$

Appendix B: The one-loop sim expressions for the HV amplitudes in SM and MSSM

Assuming CP conservation implying (8), which for the Helicity Violating (HV) amplitudes enforces the relation

$$F_{-+}(\theta) = F_{--}(\pi - \theta) \quad , \quad F_{++}(\theta) = F_{+-}(\pi - \theta) \quad , \tag{B.1}$$

we end up with the two independent HV amplitudes

$$F_{--} = F_{--}^{\text{Born}} + \alpha^2 m_W \left[\frac{u\sqrt{2}}{\sqrt{s}} N_1^L + \frac{ut}{\sqrt{2}s} (N_3^L - N_4^L) \right] \quad , \tag{B.2}$$

$$F_{+-} = F_{+-}^{\text{Born}} + \alpha^2 m_W \left[\frac{t\sqrt{2}}{\sqrt{s}} N_1^R - \frac{ut}{\sqrt{2}s} (N_3^R - N_4^R) \right] \quad , \tag{B.3}$$

expressed in terms of the Born amplitudes in (9) and the quantities $N_1^L, N_3^L - N_4^L$ and $N_1^R, N_3^R - N_4^R$ given below.

Since the HV amplitudes are vanishing at high energies though, (albeit rather slowly, like M/\sqrt{s} , as we have seen in the main text) the mass depended corrections in the augmented Sudakov terms (A.1, A.2) can often be suppressed, and a common mass scale M may be used in the logarithms, leading to the simplification

$$\begin{aligned}\overline{\ln s} &= \ln \frac{-s - i\epsilon}{M^2} , \\ \overline{\ln^2 s} &= \ln^2 \frac{-s - i\epsilon}{M^2} .\end{aligned}\tag{B.4}$$

In cases this is not sufficient though, the complete augmented Sudakov forms of Appendix A, as well as (A.3, A.4) are used. We thus obtain

in SM

$$\begin{aligned}sN_1^L &= \frac{(2s_W^2 - 1)}{2s_W^2 c_W^3} \left\{ \frac{1}{4s_W^2 c_W^2} [-\overline{\ln^2 s} + 3\overline{\ln s} - 1] + \frac{1}{2s_W^2 (2s_W^2 - 1)} [-\overline{\ln^2 s} + 3\overline{\ln s} - 1] \right. \\ &\quad \left. - \frac{c_W^2}{s_W^2 (2s_W^2 - 1)} [\overline{\ln s} + 1 + 4\overline{\ln s}] \right\} + \frac{(1 - 2s_W^2)m_H^2}{8c_W^3 s_W^4 m_W^2} (1 - \overline{\ln s}) \\ &\quad + \frac{1}{2s_W^4 c_W} \overline{\ln^2 s} - \frac{(1 + 9c_W^4 + 13c_W^6)}{8s_W^4 c_W^5} \overline{\ln s} - \frac{(1 - 2c_W^4 - 2c_W^6)}{8s_W^4 c_W^6} \\ &\quad + \frac{6}{s_W c_W} \left[\frac{m_t^2}{m_W^2} C_t^R + \frac{m_b^2}{m_W^2} C_b^R \right] + \left[\frac{2s_W^2 - 1}{2s_W^4 c_W} + \frac{(2s_W^2 - 1)^3}{4s_W^4 c_W^5} \right] \left[\frac{s\overline{\ln t}}{t} + \frac{s\overline{\ln u}}{u} \right] \\ &\quad - \frac{c_W}{2s_W^4} \left[\frac{(t - 2s)}{2t} \overline{\ln^2 t} + \frac{(u - 2s)}{2u} \overline{\ln^2 u} + \frac{(2s - u)}{2u} \overline{\ln^2 r_{ts}} + \frac{(2s - t)}{2t} \overline{\ln^2 r_{us}} \right] \\ &\quad + \frac{1}{4c_W s_W^2} \left[-\overline{\ln^2 t} - \overline{\ln^2 u} + \overline{\ln^2 r_{ts}} + \overline{\ln^2 r_{us}} \right] \\ &\quad - \left(\frac{1}{4c_W s_W^4} + \frac{(2s_W^2 - 1)^3}{8c_W^5 s_W^4} \right) \left[\frac{s\overline{\ln^2 t}}{t} + \frac{s\overline{\ln^2 u}}{u} + 2\overline{\ln^2 r_{tu}} \right] ,\end{aligned}\tag{B.5}$$

with

$$\begin{aligned}C_t^L &= \frac{(-9 + 18s_W^2 + 8s_W^4)}{72s_W^3 c_W^3} \left[\frac{\overline{\ln^2 s}}{4} - \frac{\overline{\ln s}}{2} + 1 \right] - \frac{s_W}{18c_W^3} \overline{\ln s} , \\ C_b^L &= \frac{(-9 + 18s_W^2 - 4s_W^4)}{72s_W^3 c_W^3} \left[\frac{\overline{\ln^2 s}}{4} - \frac{\overline{\ln s}}{2} + 1 \right] + \frac{s_W}{36c_W^3} \overline{\ln s} ,\end{aligned}\tag{B.6}$$

and

$$s(N_3^L - N_4^L) = -\frac{2c_W}{s_W^4} \left[\frac{(t - u)}{2tu} \overline{\ln^2 s} + \frac{\overline{\ln^2 t}}{4t} - \frac{\overline{\ln^2 u}}{4u} \right]$$

$$\begin{aligned}
& + \frac{s \overline{\ln r_{tu}}}{ut} + \frac{(2u^2 - 2t^2 + ut) \overline{\ln^2 r_{ts}}}{4tu^2} + \frac{(2u^2 - 2t^2 - ut) \overline{\ln^2 r_{us}}}{4ut^2} \Big] \\
& + \frac{1}{2c_W s_W^2} \left[\frac{\overline{\ln^2 u}}{u} - \frac{\overline{\ln^2 t}}{t} + \frac{\overline{\ln^2 r_{us}}}{t} - \frac{\overline{\ln^2 r_{ts}}}{u} \right] \\
& - \left[\frac{1}{2c_W s_W^4} + \frac{(2s_W^2 - 1)^3}{4c_W^5 s_W^4} \right] \left[\frac{s}{ut} (\overline{\ln^2 t} - \overline{\ln^2 u}) \right. \\
& \left. + \frac{2s}{ut} (\overline{\ln u} - \overline{\ln t}) + \frac{\overline{\ln^2 r_{tu}}}{u} - \frac{\overline{\ln^2 r_{tu}}}{t} \right] , \tag{B.7}
\end{aligned}$$

$$\begin{aligned}
sN_1^R &= \frac{-1}{c_W^5} \left[-\overline{\ln^2 s} + 3\overline{\ln s} - 1 \right] + \frac{\overline{\ln^2 s}}{c_W s_W^2} - \frac{\overline{\ln s}}{4c_W^5 s_W^2} (1 + 2c_W^2 + 4c_W^2) \\
& + \frac{1}{4c_W^5 s_W^2} [1 + 2c_W^2 + 4c_W^2] + \frac{(1 - 2s_W^2)m_H^2}{4c_W^3 s_W^2 m_W^2} (1 - \overline{\ln s}) \\
& + \frac{6s_W}{c_W} \left[\frac{m_t^2}{s_W^2 m_W^2} C_t^R + \frac{m_b^2}{s_W^2 m_W^2} C_b^R \right] \\
& + \frac{2s_W^2}{c_W^5} \left[\frac{s \overline{\ln t}}{t} + \frac{s \overline{\ln u}}{u} \right] - \frac{s_W^2}{c_W^5} \left[\frac{s \overline{\ln^2 t}}{t} + \frac{s \overline{\ln^2 u}}{u} + 2\overline{\ln^2 r_{tu}} \right] , \tag{B.8}
\end{aligned}$$

with

$$\begin{aligned}
C_t^R &= \frac{(-3 + 20s_W^2)}{36s_W c_W^3} \left[\frac{\overline{\ln^2 s}}{4} - \frac{\overline{\ln s}}{2} + 1 \right] + \frac{(6 - 10s_W^2)}{36s_W c_W^3} \overline{\ln s} , \\
C_b^R &= \frac{(3 + 2s_W^2)}{36s_W c_W^3} \left[\frac{\overline{\ln^2 s}}{4} - \frac{\overline{\ln s}}{2} + 1 \right] + \frac{(3 - s_W^2)}{36s_W c_W^3} \overline{\ln s} , \tag{B.9}
\end{aligned}$$

and

$$s(N_3^R - N_4^R) = -\frac{2s_W^2}{c_W^5} \left[\frac{s(\overline{\ln^2 t} - \overline{\ln^2 u})}{ut} + 2s \left(\frac{\overline{\ln u} - \overline{\ln t}}{ut} \right) + \frac{\overline{\ln^2 r_{tu}}}{u} - \frac{\overline{\ln^2 r_{tu}}}{t} \right] . \tag{B.10}$$

Correspondingly in MSSM, using the parameters in Table B.1 for $H = h^0, H^0$, and the sfermion couplings⁴

$$f_{Z\bar{f}} = -\frac{1}{s_W c_W} (I_{\bar{f}}^3 - s_W^2 Q_{\bar{f}}) , \tag{B.11}$$

$$f_{H\bar{f}} = \frac{m_W}{s_W c_W^2} (I_{\bar{f}}^3 - s_W^2 Q_{\bar{f}}) C_H^+ - \frac{m_f^2}{s_W m_W} f_{fH} , \tag{B.12}$$

⁴In (B.12), the Higgs-fermion coupling in the last two lines of Table B.1 are used.

Table B.1: Parameters for the HV amplitudes in MSSM

	h^0	H^0
C_H^-	$\sin(\beta - \alpha)$	$\cos(\beta - \alpha)$
C_H^+	$\sin(\beta + \alpha)$	$-\cos(\beta + \alpha)$
$f_{G^+G^-H}$	$\frac{m_W}{2s_W c_W^2} \cos(2\beta) \sin(\beta + \alpha)$	$-\frac{m_W}{2s_W c_W^2} \cos(2\beta) \cos(\beta + \alpha)$
$f_{H^+H^-H}$	$-\frac{m_W}{s_W} \left[\frac{\cos(2\beta) \sin(\beta + \alpha)}{2c_W^2} + \sin(\beta - \alpha) \right]$	$\frac{m_W}{s_W} \left[\frac{\cos(2\beta) \cos(\beta + \alpha)}{2c_W^2} - \cos(\beta - \alpha) \right]$
f_{tH}	$\frac{\cos \alpha}{\sin \beta}$	$\frac{\sin \alpha}{\sin \beta}$
f_{bH}	$-\frac{\sin \alpha}{\cos \beta}$	$\frac{\cos \alpha}{\cos \beta}$

we get

$$\begin{aligned}
 sN_1^L = & \frac{(2s_W^2 - 1)}{2s_W^2 c_W^3} \left\{ \frac{[-\overline{\ln^2 s_{Zee}} + 3\overline{\ln s_{Ze}(e)} - 1]}{4s_W^2 c_W^2} + \frac{[-\overline{\ln^2 s_{W\nu e}} + 3\overline{\ln s_{W\nu}(e)} - 1]}{2s_W^2(2s_W^2 - 1)} \right. \\
 & - \frac{c_W^2 [\overline{\ln s_{W\nu}(e)} + 1 + 4\overline{\ln s_{WW}(Z)}]}{s_W^2(2s_W^2 - 1)} - \sum_i Z_{1i}^+ Z_{1i}^{+*} \frac{[\overline{\ln s_{\chi_i \tilde{\nu}_{eL}}(e)} - 1]}{2s_W^2(2s_W^2 - 1)} \\
 & \left. - \sum_i \frac{|Z_{1i}^N s_W + Z_{2i}^N c_W|^2}{4s_W^2 c_W^2} [\overline{\ln s_{\chi_i \tilde{e}_L}(e)} - 1] + \sum_i \frac{c_W^2 |Z_{1i}^+|^2}{s_W^2(2s_W^2 - 1)} [\overline{\ln s_{\chi_i \tilde{\nu}_{eL}}(e)} + 1] \right\} \\
 & + C_H^- \left\{ \frac{1}{2s_W^4 c_W} \overline{\ln^2 s} - \frac{1 + 9c_W^4 + 13c_W^6}{8s_W^4 c_W^5} \overline{\ln s} - \frac{1 - 2c_W^4 - 2c_W^6}{8s_W^4 c_W^6} \right\} \\
 & - \frac{(f_{G^+G^-H} + f_{H^+H^-H})(1 - 2s_W^2)}{4c_W^3 s_W^3 m_W} (1 - \overline{\ln s}) + \frac{6s_W}{c_W} \left[\frac{m_t^2}{s_W^2 m_W^2} C_t^R f_{tH} + \frac{m_b^2}{s_W^2 m_W^2} C_b^R f_{bH} \right] \\
 & + C_H^- \left\{ -\frac{c_W}{2s_W^4} \left[\frac{(t-2s)}{2t} \overline{\ln^2 t} + \frac{(u-2s)}{2u} \overline{\ln^2 u} + \frac{(2s-u)}{2u} \overline{\ln^2 r_{ts}} + \frac{(2s-t)}{2t} \overline{\ln^2 r_{us}} \right] \right. \\
 & + \frac{1}{4c_W s_W^2} \left[-\overline{\ln^2 t} - \overline{\ln^2 u} + \overline{\ln^2 r_{ts}} + \overline{\ln^2 r_{us}} \right] \\
 & \left. - \left(\frac{1}{4c_W s_W^4} + \frac{(2s_W^2 - 1)^3}{8c_W^5 s_W^4} \right) \left[\frac{s}{t} \overline{\ln^2 t} + \frac{s}{u} \overline{\ln^2 u} + 2\overline{\ln^2 r_{tu}} \right] \right\} \\
 & + \left(\frac{(2s_W^2 - 1) \sin \alpha < M_{12}^+ >}{2\sqrt{2} c_W s_W^4 m_W} + \frac{(2s_W^2 - 1)^2 < M_{L+}^0 >}{8c_W^4 s_W^4 m_W} \right) \left[\frac{s \overline{\ln^2 t}}{2t} - 2 \frac{s \overline{\ln t}}{t} + \frac{s \overline{\ln^2 u}}{2u} - 2 \frac{s \overline{\ln u}}{u} \right] \\
 & + \left(\frac{1 - 2s_W^2}{4c_W^3 s_W^4} - \frac{(1 - 2s_W^2)^2}{8c_W^5 s_W^4} \right) C_H^+ \left[\frac{s \overline{\ln t}}{t} + \frac{s \overline{\ln u}}{u} \right] \\
 & + \frac{2}{m_W} \Sigma_{\tilde{f}} f_{Z\tilde{f}} f_{H\tilde{f}} \left[Q_{\tilde{f}} + \frac{2s_W^2 - 1}{2s_W c_W} f_{Z\tilde{f}} \right] (1 - \overline{\ln s}) \\
 & - \frac{\sqrt{2}}{m_W} \left\{ \frac{(1 - 4c_W^2)}{s_W^2 c_W} (< M_{21}^+ > \cos \alpha - < M_{12}^+ > \sin \alpha) \left[\frac{1}{4} \overline{\ln^2 s} - \overline{\ln s} + 1 \right] \right. \\
 & \left. - \frac{(1 - 2s_W^2)}{4s_W^4 c_W^3} \left[2c_W^2 (1 - 2s_W^2) (< M_{21}^+ > \cos \alpha - < M_{12}^+ > \sin \alpha) \overline{\ln s} \right] \right\}
 \end{aligned}$$

$$\begin{aligned}
& -(8c_W^4 - 4c_W^2 - 1)(\langle M_{21}^+ \rangle \cos \alpha - \langle M_{12}^+ \rangle \sin \alpha) \left(\frac{1}{4} \overline{\ln^2 s} - \frac{1}{2} \overline{\ln s} + 1 \right) \Big] \Big\} \\
& - \frac{(1 - 2s_W^2)}{4s_W^4 c_W^4 m_W} \langle M_{L-}^0 \rangle \left[\frac{1}{4} \overline{\ln^2 s} - \frac{1}{2} \overline{\ln s} + 1 \right] \\
& - \left(\frac{1}{8c_W^3 s_W^4} + \frac{(1 - 2s_W^2)^2}{16s_W^4 c_W^5} \right) C_H^+ \left[\frac{s}{u} \overline{\ln^2 r_{ts}} + \frac{s}{t} \overline{\ln^2 r_{us}} \right] \\
& - \frac{\langle M_{12}^+ \rangle c_W \sin \alpha}{2\sqrt{2}s_W^4 m_W} \left[\overline{\ln^2 t} + \overline{\ln^2 u} + \frac{t}{u} \overline{\ln^2 r_{ts}} + \frac{u}{t} \overline{\ln^2 r_{us}} \right. \\
& \left. - 2\overline{\ln^2 s} - \frac{s}{u} \overline{\ln^2 r_{ts}} - \frac{s}{t} \overline{\ln^2 r_{us}} + \frac{(1 - 2s_W^2)}{2c_W^2} (-\overline{\ln^2 t} - \overline{\ln^2 u} + \overline{\ln^2 r_{ts}} + \overline{\ln^2 r_{us}}) \right] \\
& + \frac{(1 - 2s_W^2) \langle M_{L-}^0 \rangle}{16s_W^4 c_W^4 m_W} [-\overline{\ln^2 t} + \overline{\ln^2 r_{ts}} - \overline{\ln^2 u} + \overline{\ln^2 r_{us}}] \\
& + \frac{\sin \alpha}{2\sqrt{2}s_W^4 c_W} \frac{\langle M_{12}^+ \rangle}{m_W} \overline{\ln^2 r_{tu}} + \frac{(1 - 2s_W^2)^2 \langle M_{L+}^0 \rangle}{8s_W^4 c_W^4 m_W} \overline{\ln^2 r_{tu}} , \tag{B.13}
\end{aligned}$$

$$\begin{aligned}
s(N_3^L - N_4^L) &= C_H^- \left\{ -\frac{2c_W}{s_W^4} \left[\frac{(t-u)}{2tu} \overline{\ln^2 s} + \frac{\overline{\ln^2 t}}{4t} - \frac{\overline{\ln^2 u}}{4u} \right. \right. \\
&+ \frac{s \overline{\ln r_{tu}}}{ut} + \frac{(2u^2 - 2t^2 + ut)}{4tu^2} \overline{\ln^2 r_{ts}} + \frac{(2u^2 - 2t^2 - ut)}{4ut^2} \overline{\ln^2 r_{us}} \Big] \\
&+ \frac{1}{2c_W s_W^2} \left[\frac{\overline{\ln^2 u}}{u} - \frac{\overline{\ln^2 t}}{t} + \frac{\overline{\ln^2 r_{us}}}{t} - \frac{\overline{\ln^2 r_{ts}}}{u} \right] \\
&- \left(\frac{1}{2c_W s_W^4} + \frac{(2s_W^2 - 1)^3}{4c_W^5 s_W^4} \right) \left[\frac{s}{ut} (\overline{\ln^2 t} - \overline{\ln^2 u}) + \frac{2s}{ut} (\overline{\ln u} - \overline{\ln t}) + \frac{\overline{\ln^2 r_{tu}}}{u} - \frac{\overline{\ln^2 r_{tu}}}{u} \right] \Big\} \\
&- \left(\frac{1}{4c_W^3 s_W^4} + \frac{(2s_W^2 - 1)^2}{8s_W^4 c_W^5} \right) C_H^+ \left[\frac{s \overline{\ln^2 r_{ts}}}{u^2} - \frac{s \overline{\ln^2 r_{us}}}{t^2} + 2s \frac{\overline{\ln r_{ts}} - \overline{\ln r_{us}}}{ut} \right] \\
&- \frac{\langle M_{12}^+ \rangle c_W \sin \alpha}{\sqrt{2}s_W^4 m_W} \left[\frac{\overline{\ln^2 s}}{t} - \frac{\overline{\ln^2 s}}{u} + \frac{\overline{\ln^2 u}}{u} - \frac{\overline{\ln^2 t}}{t} - \frac{2s \overline{\ln r_{ts}}}{ut} \right. \\
&+ \frac{2s \overline{\ln r_{us}}}{ut} + \frac{t}{u^2} \overline{\ln^2 r_{us}} - \frac{u}{t^2} \overline{\ln^2 r_{us}} + \frac{s(u-t)}{tu^2} \overline{\ln^2 r_{ts}} + \frac{s(u-t)}{ut^2} \overline{\ln^2 r_{us}} \\
&+ \frac{(1 - 2s_W^2)}{2c_W^2} \left(\frac{\overline{\ln^2 t}}{t} - \frac{\overline{\ln^2 u}}{u} + \frac{\overline{\ln^2 r_{ts}}}{u} - \frac{\overline{\ln^2 r_{us}}}{t} \right) \Big] + \frac{C_H^+}{s_W^4} \left(\frac{s}{tu} \right) \overline{\ln r_{tu}} \\
&+ \frac{(1 - 2s_W^2) \langle M_{L-}^0 \rangle}{8s_W^4 c_W^4 m_W} \left(\frac{\overline{\ln^2 t}}{t} + \frac{\overline{\ln^2 r_{ts}}}{u} - \frac{\overline{\ln^2 u}}{u} - \frac{\overline{\ln^2 r_{us}}}{t} \right) \\
&+ \left[\frac{\langle M_{12}^+ \rangle \sin \alpha}{\sqrt{2}s_W^4 c_W m_W} + \frac{(1 - 2s_W^2)^2 \langle M_{L+}^0 \rangle}{4s_W^4 c_W^4 m_W} \right] \left[\frac{s(\overline{\ln^2 t} - \overline{\ln^2 u})}{2tu} \right. \\
&\left. - \frac{2s \overline{\ln^2 r_{tu}}}{tu} + \frac{\overline{\ln^2 r_{tu}}}{2u} - \frac{\overline{\ln^2 r_{tu}}}{2t} \right] , \tag{B.14}
\end{aligned}$$

$$\begin{aligned}
sN_1^R = & \frac{-1}{c_W^3} \left\{ \frac{[-\overline{\ln^2 s_{Ze}} + 3\overline{\ln s_{Ze}(e)} - 1]}{c_W^2} - \sum_i \frac{|Z_{1i}^N|^2}{c_W^2} [\overline{\ln s_{\chi_i \tilde{e}_R}(e)} - 1] \right\} \\
& + C_H^- \left\{ \frac{\overline{\ln^2 s}}{c_W s_W^2} - \frac{\overline{\ln s}}{4c_W^5 s_W^2} [1 + 2c_W^2 + 4c_W^2] + \frac{1}{4c_W^5 s_W^2} [1 + 2c_W^2 + 4c_W^2] \right\} \\
& - \frac{f_{G^+ G^- H}(1 - 2s_W^2)}{2c_W^3 s_W m_W} (1 - \overline{\ln s}) + \frac{6s_W}{c_W} \left[\frac{m_t^2}{s_W^2 m_W^2} C_t^R f_{tH} + \frac{m_b^2}{s_W^2 m_W^2} C_b^R f_{bH} \right] \\
& + C_H^- \left\{ \frac{2s_W^2}{c_W^5} \left[\frac{\overline{s \ln t}}{t} + \frac{\overline{s \ln u}}{u} \right] - \frac{s_W^2}{c_W^5} \left[\frac{\overline{s \ln^2 t}}{t} + \frac{\overline{s \ln^2 u}}{u} + 2\overline{\ln^2 r_{tu}} \right] \right\} \\
& + \frac{s_W < M_{R+}^0 >}{c_W^4 m_W} \left[\frac{\overline{s \ln^2 t}}{2t} - 2\frac{\overline{s \ln t}}{t} + \frac{\overline{s \ln^2 u}}{2u} - 2\frac{\overline{s \ln u}}{u} \right] + \frac{2s_W^2}{c_W^5} C_H^+ \left[\frac{\overline{s \ln t}}{t} + \frac{\overline{s \ln u}}{u} \right] \\
& + \frac{2}{m_w} \Sigma_{\tilde{f}} f_{Z\tilde{f}} f_{H\tilde{f}} \left[Q_{\tilde{f}} + \frac{s_W}{c_W} f_{Z\tilde{f}} \right] (1 - \overline{\ln s}) \\
& - \frac{\sqrt{2}}{m_W} \left\{ \frac{(1 - 4c_W^2)}{s_W^2 c_W} (< M_{21}^+ > \cos \alpha - < M_{12}^+ > \sin \alpha) \left[\frac{1}{4} \overline{\ln^2 s} - \overline{\ln s} + 1 \right] \right. \\
& + \frac{1}{2s_W^2 c_W^3} \left[2c_W^2 (1 - 2s_W^2) (< M_{21}^+ > \cos \alpha - < M_{12}^+ > \sin \alpha) \overline{\ln s} \right. \\
& \left. \left. - (8c_W^4 - 4c_W^2 - 1) (< M_{21}^+ > \cos \alpha - < M_{12}^+ > \sin \alpha) \left(\frac{1}{4} \overline{\ln^2 s} - \frac{1}{2} \overline{\ln s} + 1 \right) \right] \right\} \\
& + \frac{1}{2s_W^2 c_W^4 m_W} < M_{L-}^0 > \left[\frac{1}{4} \overline{\ln^2 s} - \frac{1}{2} \overline{\ln s} + 1 \right] \\
& - \frac{< M_{R-}^0 >}{4s_W c_W^4 m_W} [-\overline{\ln^2 t} + \overline{\ln^2 r_{ts}} - \overline{\ln^2 u} + \overline{\ln^2 r_{us}}] \\
& + \frac{s_W^2}{c_W^5} C_H^+ \left[\frac{\overline{s \ln^2 r_{ts}}}{u} + \frac{\overline{s \ln^2 r_{us}}}{t} \right] + \frac{s_W < M_{R+}^0 >}{c_W^4 m_W} \overline{\ln^2 r_{us}} , \tag{B.15}
\end{aligned}$$

$$\begin{aligned}
s(N_3^R - N_4^R) = & -\frac{2s_W^2}{c_W^5} C_H^- \left[\frac{\overline{\ln^2 t} - \overline{\ln^2 u}}{ut} + 2 \left(\frac{\overline{\ln u} - \overline{\ln t}}{ut} \right) + \frac{\overline{\ln^2 r_{tu}}}{su} - \frac{\overline{\ln^2 r_{tu}}}{st} \right] \\
& + \frac{2s_W^2}{c_W^5} C_H^+ \left[\frac{\overline{\ln^2 r_{ts}}}{u^2} - \frac{\overline{\ln^2 r_{us}}}{t^2} + 2 \frac{\overline{\ln r_{ts}} - \overline{\ln r_{us}}}{ut} \right] \\
& - \frac{< M_{R-}^0 >}{2s_W c_W^4 m_W} \left[\frac{\overline{\ln^2 t}}{t} - \frac{\overline{\ln^2 u}}{u} + \frac{\overline{\ln^2 r_{ts}}}{u} - \frac{\overline{\ln^2 r_{us}}}{t} \right] \\
& + \frac{s_W < M_{R+}^0 >}{c_W^4 m_W} \left[\frac{\overline{s \ln^2 t}}{ut} - \frac{\overline{s \ln^2 u}}{ut} - 4s \frac{\overline{\ln r_{tu}}}{ut} + \frac{\overline{\ln^2 r_{tu}}}{u} - \frac{\overline{\ln^2 r_{tu}}}{t} \right] . \tag{B.16}
\end{aligned}$$

In (B.13-B.16) some mass averages appear, which for h^0 are

$$< M_{12}^+ > = \frac{m_W \sqrt{2}}{\sqrt{1 + \tan^2 \beta}} , \quad < M_{21}^+ > = \frac{m_W \sqrt{2} \tan \beta}{\sqrt{1 + \tan^2 \beta}} ,$$

$$\begin{aligned}
M_{L+}^0 &= \sin \alpha (s_W M_{13}^N + c_W M_{23}^N) + \cos \alpha (s_W M_{14}^N + c_W M_{24}^N) \quad , \\
M_{L-}^0 &= -\sin \alpha (s_W M_{13}^N + c_W M_{23}^N) + \cos \alpha (s_W M_{14}^N + c_W M_{24}^N) \quad , \\
M_{R-}^0 &= \sin \alpha M_{13}^N - \cos \alpha M_{14}^N \quad , \\
M_{R+}^0 &= \sin \alpha M_{13}^N + \cos \alpha M_{14}^N \quad , \\
M_{L-}'^0 &= \sin \alpha (s_W M_{13}^N - c_W M_{23}^N) + \cos \alpha (s_W M_{14}^N - c_W M_{24}^N) \quad , \\
M_{13}^N &= \frac{-m_W c_W}{s_W \sqrt{1 + \tan^2 \beta}} \quad , \quad M_{23}^N = \frac{m_W}{\sqrt{1 + \tan^2 \beta}} \quad , \\
M_{14}^N &= \frac{m_W s_W \tan \beta}{c_W \sqrt{1 + \tan^2 \beta}} \quad , \quad M_{24}^N = \frac{-m_W \tan \beta}{\sqrt{1 + \tan^2 \beta}} \quad ,
\end{aligned} \tag{B.17}$$

while the corresponding expressions for H^0 may be obtained from them by replacing

$$\sin \alpha \rightarrow -\cos \alpha \quad , \quad \cos \alpha \rightarrow \sin \alpha \quad . \tag{B.18}$$

B.1 A simpler approximation for the HV amplitudes

As the HV amplitudes are less important than the HC ones, we can try an even simpler approximation at intermediate energies, by neglecting mass differences and using a common mass-scale m_W . Thus at energies like e.g. in the range 0.6-5 TeV, we try fitting the complete Born+1loop contributions by a Sudakov-type expression⁵ of the form

$$F^{\text{HV}} = F^{\text{Born}} \left\{ 1 + a \ln^2 \frac{s}{m_W^2} + b \ln \frac{s}{m_W^2} + c \right\} \quad . \tag{B.19}$$

Using this, the fitted constants are given in Table B.2 for the benchmarks S1(S2) of ref.[21].

Table B.2: Fits of the approximate expression (B.19) to the HV amplitudes for the S1 (S2) benchmarks of [21], in the energy range 0.6-5 TeV.

	SM: H			MSSM S1(S2): h^0		
	a	b	c	a	b	c
F_{--}, F_{-+}	-0.0075	0.024	-0.058	-0.015(-0.013)	0.12(0.10)	-0.28(-0.22)
F_{+-}, F_{++}	-0.0046	0.017	0.050	-0.0027(-0.0026)	-0.005(-0.008)	0.14(0.16)

⁵Although there is no rigorous Sudakov rule for such suppressed amplitudes.

References

- [1] P. Higgs, Phys. Lett. 12 (1964) 132; Phys. Rev. Lett. **13**, 508 (1964); Phys. Rev. **145**, 1156 (1966)); F. Englert and R. Brout, Phys. Rev. Lett. **13**, 321 (1964); G. Guralnik, C. Hagen and T. Kibble, Phys. Rev. Lett. **13**, 585 (1964).
- [2] G. Aad et al. [ATLAS Collaboration], Phys. Lett. **B716**, 1 (2012) [arXiv:1207.7214 [hep-ex]]. S. Chatrchyan et al. [CMS Collaboration], Phys. Lett. **B716**, 30 (2012) [arXiv:1207.7235 [hep-ex]]. Gavin J. Davies for the CDF and D0 Collaborations, published in Front.Phys.China **8**, 270 (2013), [arXiv:1207.0449 [hep-ex]]. ATLAS Collaboration, see: <https://twiki.cern.ch/twiki/bin/view/AtlasPublic/HiggsPublicResults>. CMS Collaboration, see: <https://twiki.cern.ch/twiki/bin/view/CMSPublic/PhysicsResultsHIG>.
- [3] John Ellis, 1312.5672, Higgs working group 1310.8361, Klute et al 1301.1322. A. Djouadi, Phys. Rept. **459**, 1 (2008) 1 [arXiv:hep-ph/0503173]. J. Gunion, H. Haber, G. Kane and S. Dawson, The Higgs Hunter's Guide, Addison-Wesley, 1990. S. Heinemeyer, Int. J. Mod. Phys. **A21**, 2659 (2006) [arXiv:hep-ph/0407244].
- [4] Higgs Working Group Report, A. Ajaib et al, arXiv:(hep-ex)1310.8361. T.Behnke et al, The Int.Lin.Coll.Tech.Design Report, arXiv:1306.6327.
- [5] G.J. Gounaris and F.M. Renard, Phys. Rev. Lett. **94**, 131601 (2005), hep-ph/0501046.
- [6] G.J. Gounaris and F.M. Renard, Phys. Rev. **D73**, 097301 (2006), hep-ph/0604041, (an Addendum).
- [7] G.J. Gounaris and F.M. Renard, Acta Phys. Polon. **42**, 2107 (2011), arXiv:1106.2707[hep-ph].
- [8] G.J. Gounaris and F.M. Renard, Phys. Rev. **D86**, 013003 (2012), arXiv:1205.4547 [hep-ph].
- [9] G.J. Gounaris and F.M. Renard, Phys. Rev. **D88**, 113003 (2013), arXiv:1309.3177 [hep-ph].
- [10] A. Denner, J. Kubleck, R. Mertig, M. Bohm, Z. f. Phys. **C56**, 261 (1992). B.A. Kniehl, Z. f. Phys. **C55**, 605 (1992). A. Denner , B.A. Kniehl, Nucl. Phys. Proc. Suppl. **29A**, 263 (1992). R. Hempfling, B.A. Kniehl, Z. f. Phys. **C59**, 263 (1993).
- [11] M. Beccaria, M. Melles, F. M. Renard, S. Trimarchi, C. Verzegnassi, Int. J. Mod. Phys. **A18**, 5069 (2003), hep-ph/0304110. M. Beccaria, F.M. Renard and C. Verzegnassi, Nucl.Phys. B663 (2003) 394, hep-ph/0304175. M. Beccaria, E. Mirabella, Phys. Rev. **D71**, 115016 (2005), [hep-ph/0505172].

- [12] J.M. Cornwall, D.N. Levin, and G. Tiktopoulos, Phys. Rev. **D10**, 1145 (1974); C.E.Vayonakis, Lett.Nuov.Cim. **17**, 383 (1976).
- [13] M.S. Chanowitz, and M.K. Gaillard, Nucl. Phys. **B261**, 379 (1985); G.J. Gounaris, R. Kögerler and H. Neufeld, Phys. Rev. **D34**, 3257 (1986).
- [14] G.J. Gounaris, F.M. Renard and N.D. Vlachos, Nucl. Phys. **B459**, 51 (1996); G.J. Gounaris, D.T. Papadamou and F.M. Renard, Z. f. Phys. **C76**, 333 (1997).
- [15] M. Jacob and G.C. Wick, Annals of Phys. **7**, 404 (1959), Annals of Phys. **281**, 774 (2000).
- [16] G. Passarino and M. Veltman Nucl. Phys. **B160**, 151 (1979).
- [17] W. Hollik, Fortsch. Phys. **38**, 165 (1990).
- [18] A. Freitas and D. Stockinger, Phys. Rev. **D66**, 095014 (2002); see also arXiv: hep-ph/0210372.
- [19] M. Beccaria, A. Ferrari, F.M. Renard, C. Verzegnassi, LC-TH-2005-005, arXiv:(hep-ph) 0506274.
- [20] M. Beccaria, G.J. Gounaris, J. Layssac and F.M. Renard, Int. J. Mod. Phys. **A23**, 1839 (2008).
- [21] M Arana-Catania, S. Heinemeyer, M.J. Herrero, Phys. Rev. **D88**, 015026 (2013) arXiv:1304.2783[hep-ph]. See also arXiv:1405.6960[hep-ph].
- [22] G. Degrassi and A. Sirlin, Nucl. Phys. **B383**, 73 (1992), Phys. Rev. **D46**, 3104 (1992).

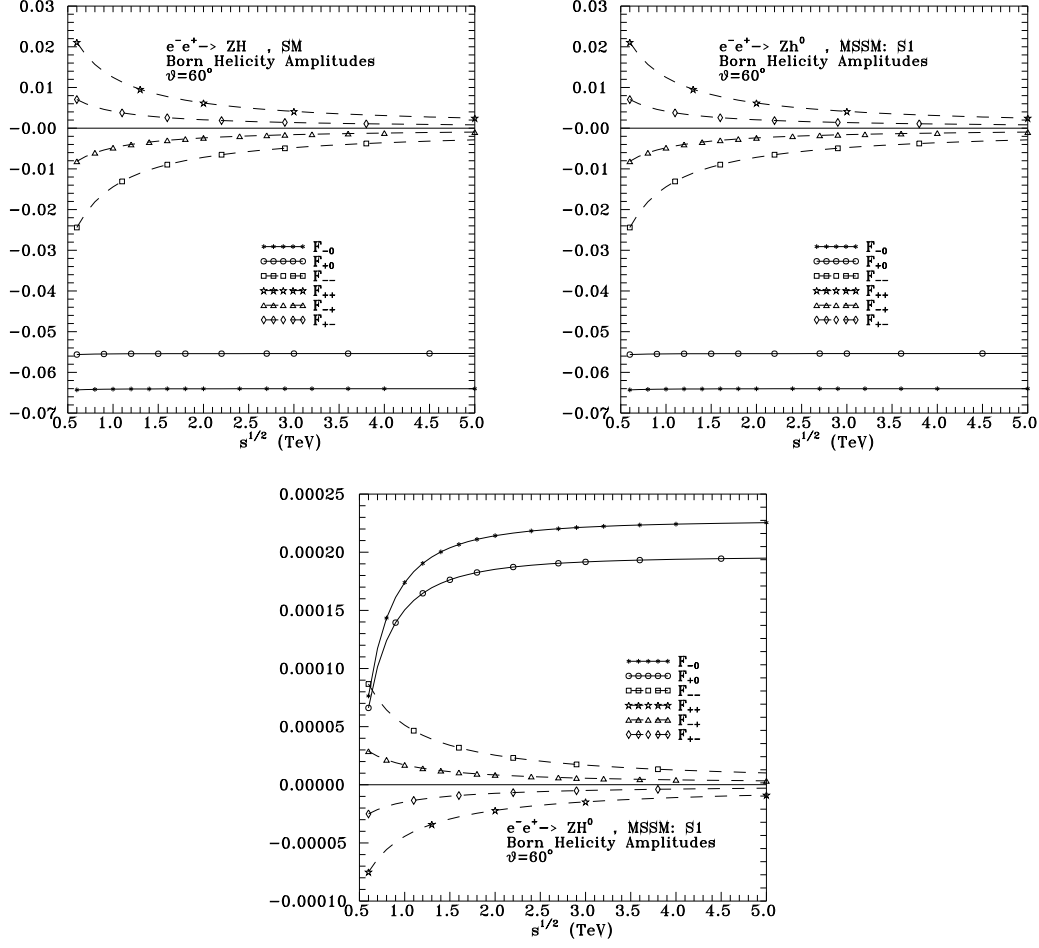


Figure 1: Energy dependence of the six Born helicity amplitudes at $\theta = 60^\circ$, for the SM processes $e^-e^+ \rightarrow ZH$ (upper left panel), and the MSSM processes $e^-e^+ \rightarrow Zh^0, ZH^0$ (upper right and the lower panels, respectively). For the SUSY cases we use the S1 MSSM benchmark of [21].

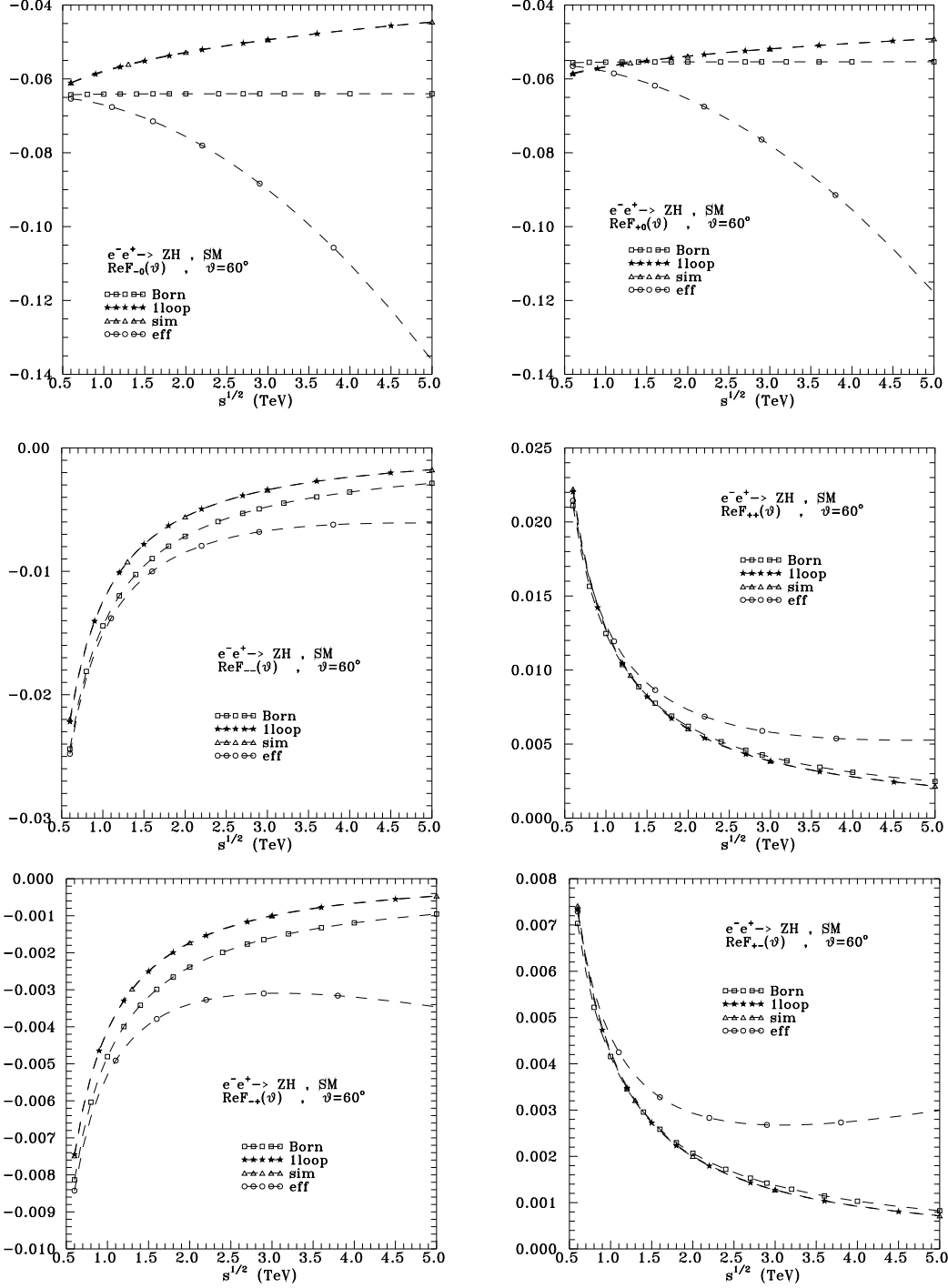


Figure 2: The six $e^-e^+ \rightarrow ZH$ SM-amplitudes at $\theta = 60^\circ$, in the Born, 1loop and sim approximations, together with amplitudes containing "eff" BSM contributions. Upper row gives the HC amplitudes, while the HV ones are shown in the lower ones.

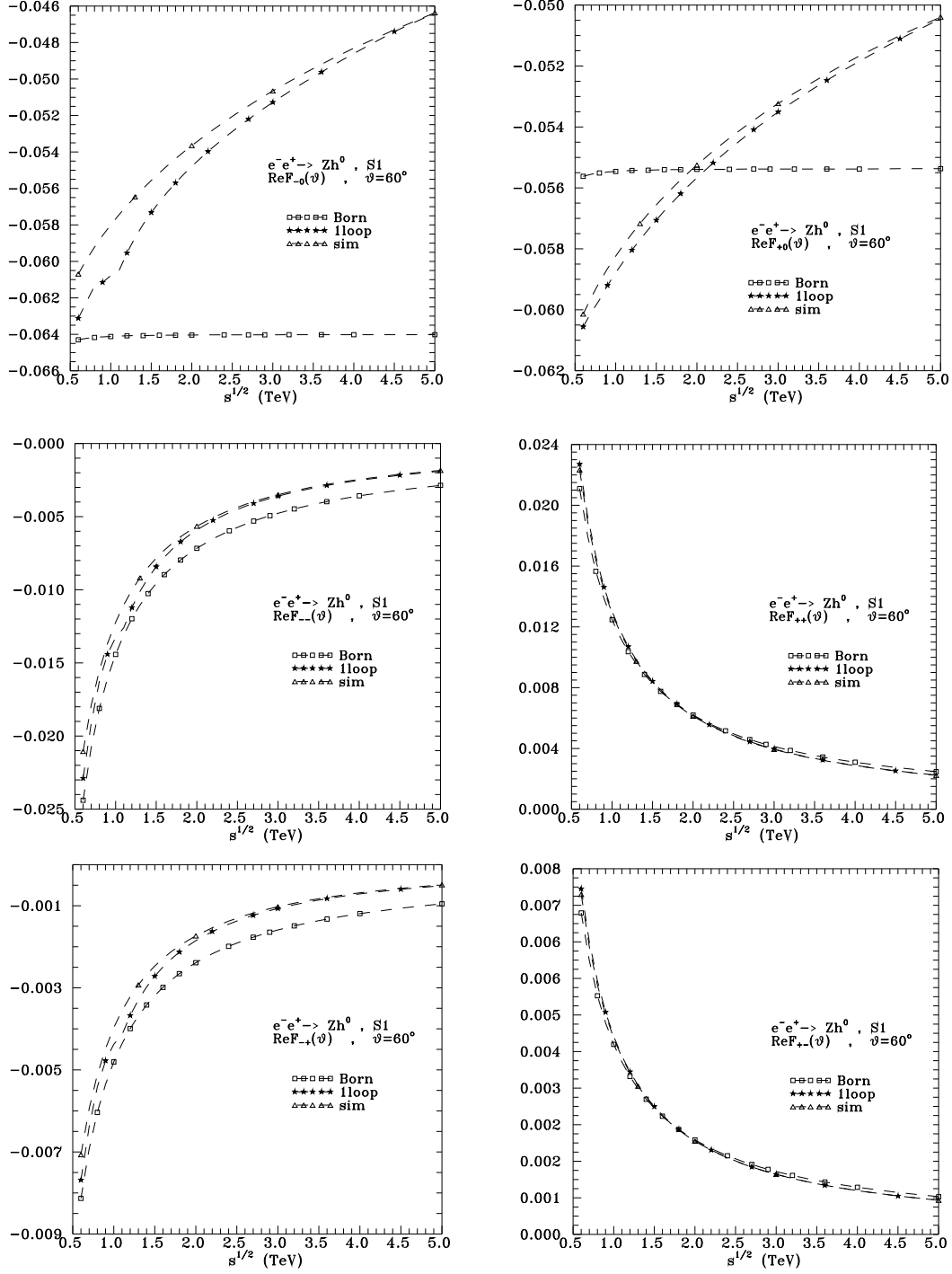


Figure 3: The six MSSM $e^-e^+ \rightarrow Zh^0$ amplitudes at $\theta = 60^\circ$, for the S1 benchmark of [21], in the Born, 1loop and sim approximations. Upper row gives the HC amplitudes, while the HV ones are shown in the lower ones.

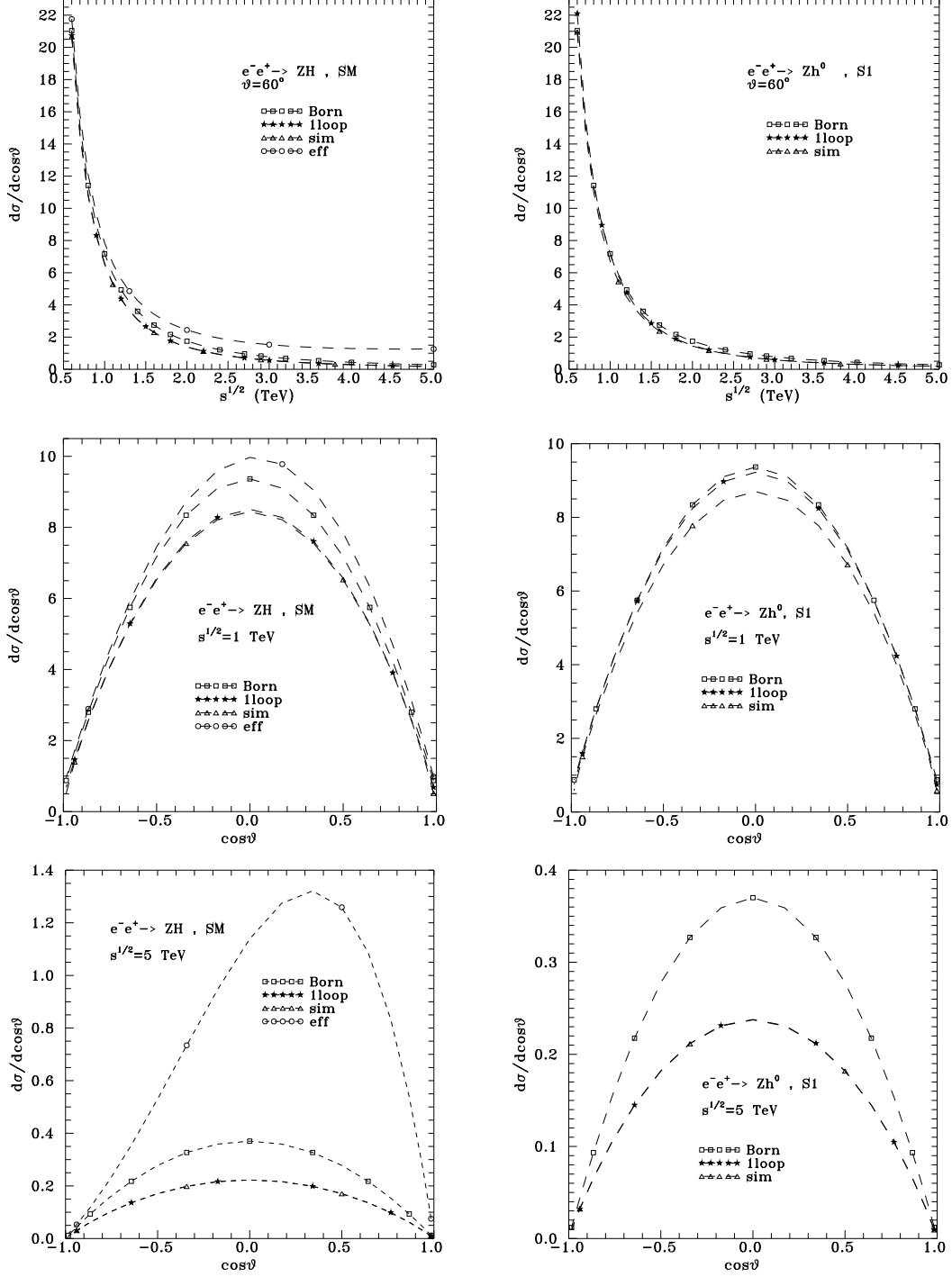


Figure 4: The unpolarized differential cross sections in SM (left panels) and the S1 MSSM benchmark [21] (right panels). Upper row describes energy dependence at $\theta = 60^\circ$; middle (lowest) panels give the angular distributions at $\sqrt{s} = 1$ TeV ($\sqrt{s} = 5$ TeV).

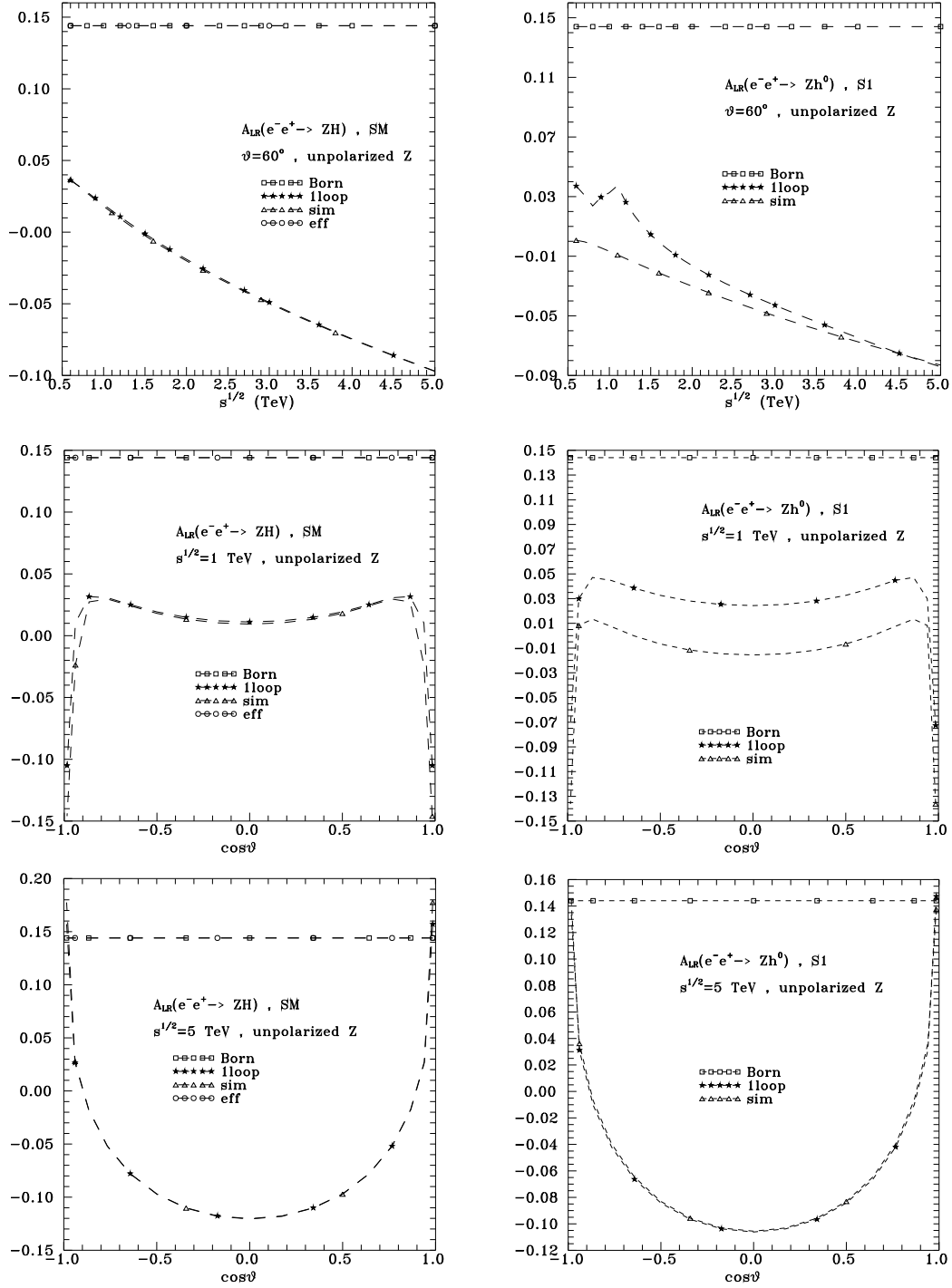


Figure 5: The A_{LR} asymmetries for unpolarized Z, as defined in (27). See caption in Fig.4.

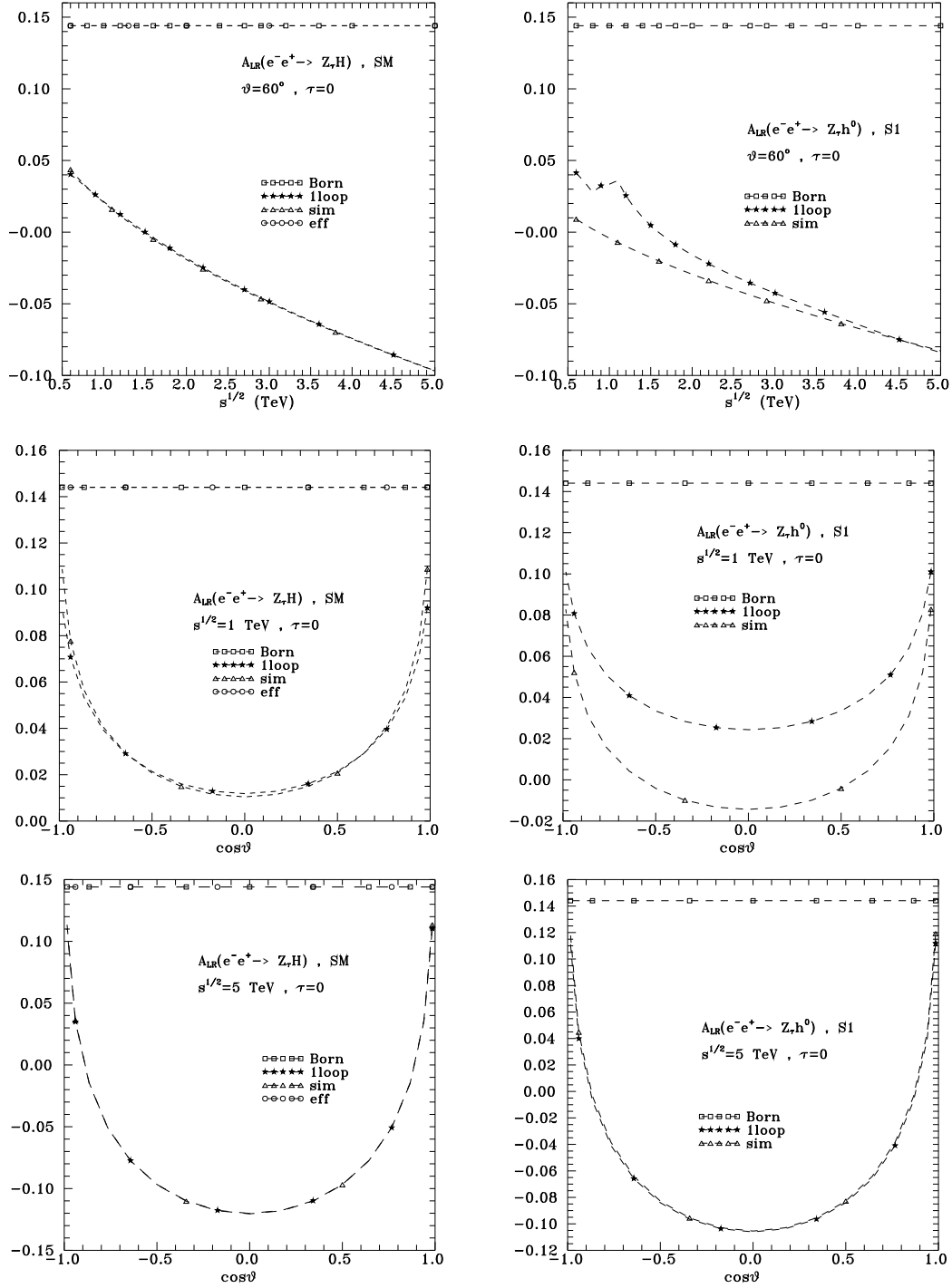


Figure 6: The A_{LR} asymmetries defined in (28), for a final Z of helicity $\tau = 0$. See caption in Fig.4.

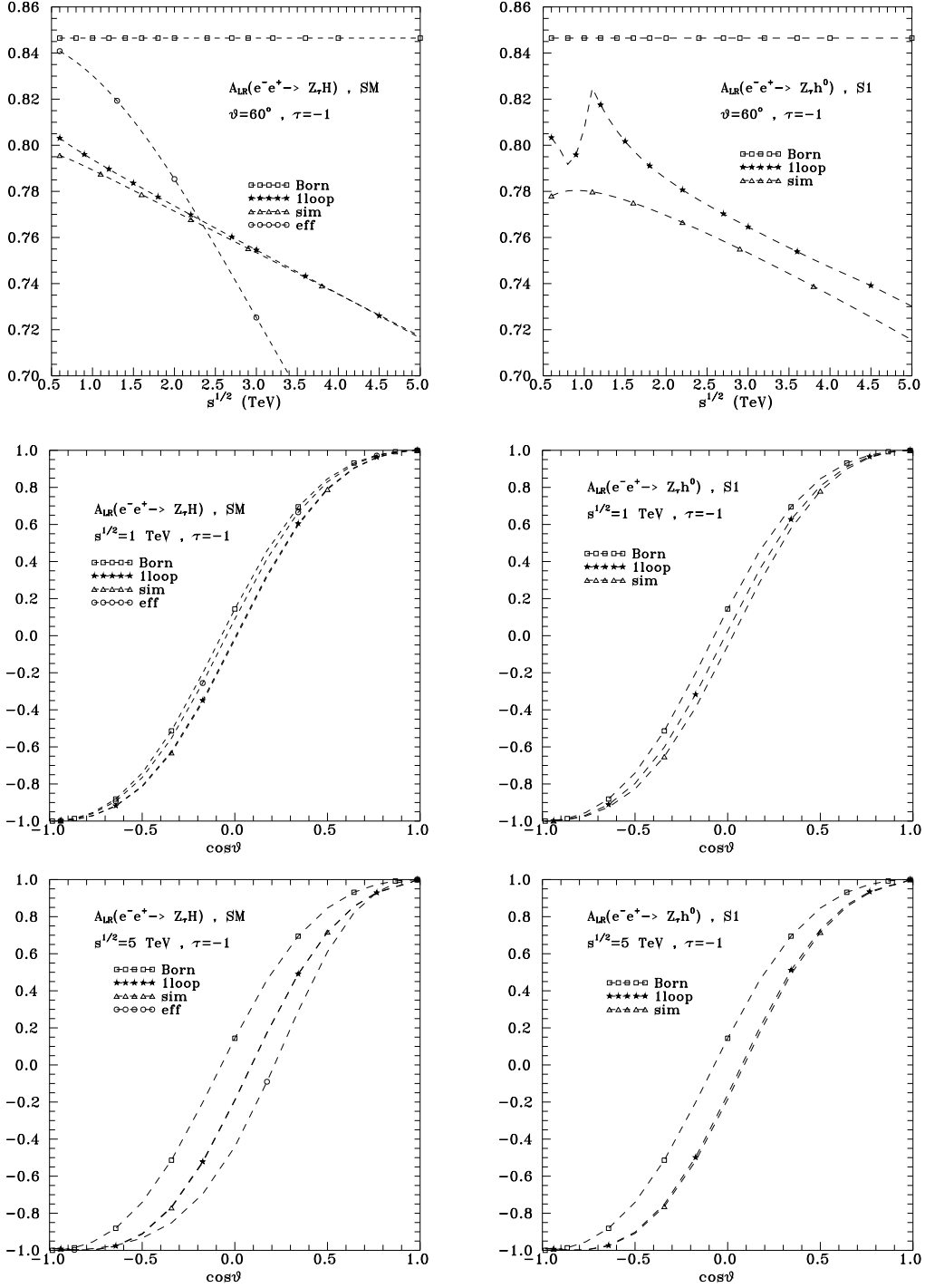


Figure 7: The A_{LR} asymmetries defined in (28), for a final Z of helicity $\tau = -1$. See caption in Fig.4

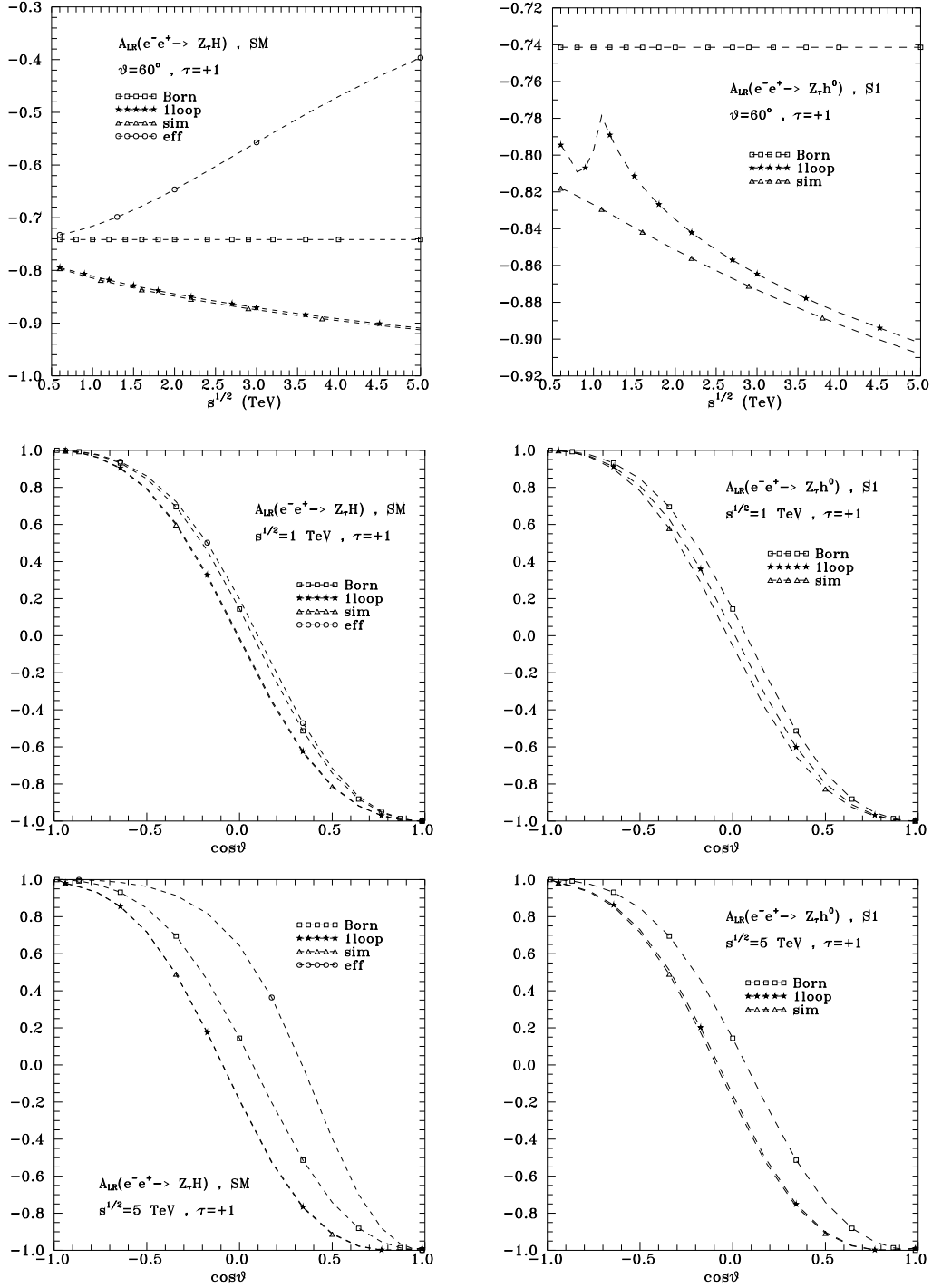


Figure 8: The A_{LR} asymmetries defined in (28), for a final Z of helicity $\tau = 1$. See caption in Fig.4.

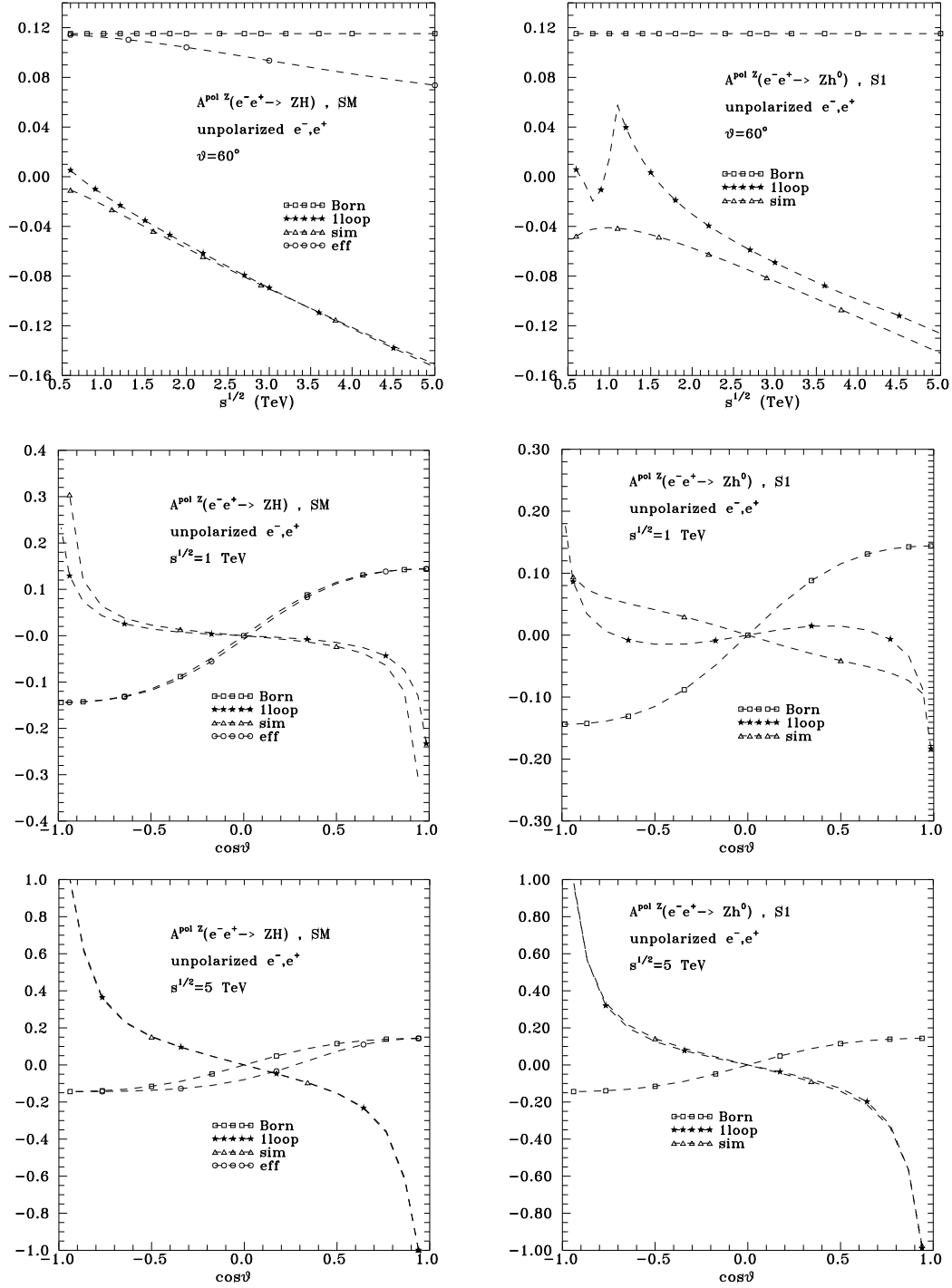


Figure 9: $A^{\text{pol } Z}$ asymmetries defined in (30), for unpolarized (e^- , e^+)-beams. See caption in Fig.4.

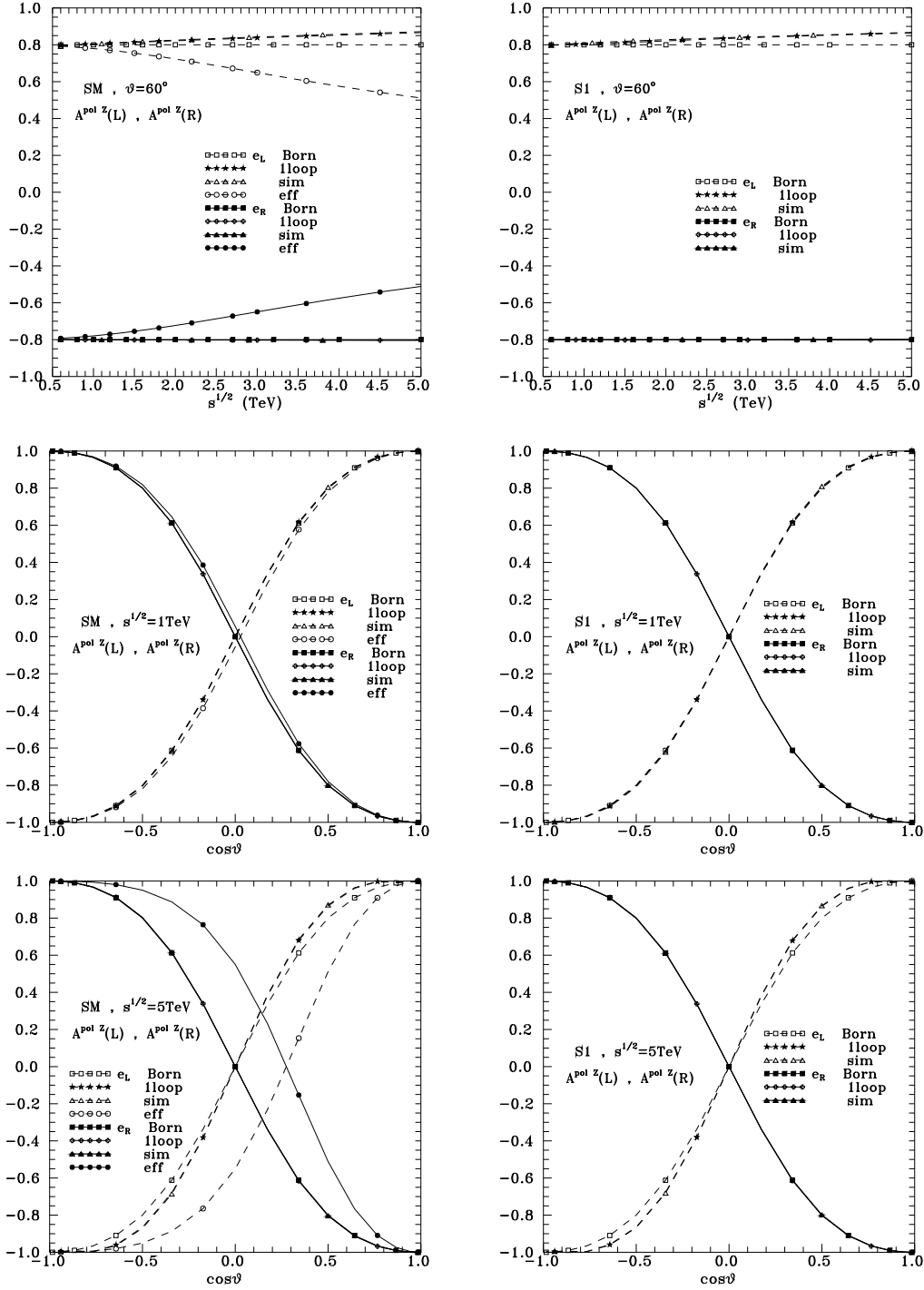


Figure 10: $A^{\text{pol } Z}(\lambda)$ asymmetries defined in (31) for e^- -beams with definite helicity $\lambda = L, R$. See caption in Fig.4.